

1 **Evidence for increased expression of the Amundsen Sea Low over the South Atlantic**
2 **during the late Holocene**

3

4 Zoë A. Thomas^{1,2,3}, Richard T. Jones[†], Chris J. Fogwill^{1,2,5}, Jackie Hatton⁴, Alan Williams^{3,6}, Alan
5 Hogg⁷, Scott Mooney¹, Philip Jones⁸, David Lister⁸, Paul Mayewski⁹ and Chris S. M. Turney^{1,2,3}

6

7 1. Palaeontology, Geobiology and Earth Archives Research Centre, School of Biological, Earth
8 and Environmental Sciences, University of New South Wales, Australia

9 2. Climate Change Research Centre, School of Biological, Earth and Environmental Sciences,
10 University of New South Wales, Australia

11 3. ARC Centre of Excellence in Australian Biodiversity and Heritage (CABAH), School of
12 Biological, Earth and Environmental Sciences, University of New South Wales, Sydney, Australia

13 4. Department of Geography, Exeter University, Devon, EX4 4RJ, United Kingdom

14 5. School of Geography, Geology and the Environment, Keele University, Staffordshire,
15 ST5 5BG, UK

16 6. Extent Heritage Pty Ltd, 3/73 Union Street, Pyrmont, NSW 2009, Australia

17 7. Waikato Radiocarbon Laboratory, University of Waikato, Private Bag 3105, Hamilton, New
18 Zealand

19 8. Climatic Research Unit, School of Environmental Sciences, University of East Anglia, Norwich,
20 UK

21 9. Climate Change Institute, University of Maine, Orono, ME, USA

22 †. Deceased.

23 * E-mail: z.thomas@unsw.edu.au

24

25

26

27

28 **Abstract:**

29 The Amundsen Sea Low (ASL) plays a major role in the climate and environment of Antarctica
30 and the Southern Ocean, including surface air temperature and sea ice concentration changes,
31 Unfortunately, a relative dearth of observational data across the Amundsen and Bellingshausen
32 Seas prior to the satellite era (post-1979) limits our understanding of past behaviour and
33 impact of the ASL. The limited proxy evidence for changes in the ASL are primarily limited to the
34 Antarctic where ice core evidence suggests a deepening of the atmospheric pressure system
35 during the late Holocene. However, no data has previously been reported from the northern
36 side of the ASL. Here we report a high-resolution, multi-proxy study of a 5000 year-long peat
37 record from the Falkland Islands, a location sensitive to contemporary ASL dynamics which
38 modulates northerly and westerly airflow across the southwestern South Atlantic sector of the
39 Southern Ocean. In combination with climate reanalysis, we find a marked period of wetter,
40 colder conditions most likely the result of enhanced southerly airflow between 5000 and 2500
41 years ago, suggesting limited ASL influence over the region. After 2500 years ago, drier and
42 warmer conditions were established, implying more westerly airflow and the increased
43 projection of the ASL onto the South Atlantic. The possible role of the equatorial Pacific via
44 atmospheric teleconnections in driving this change is discussed. Our results are in agreement
45 with Antarctic ice core records and fjord sediments from the southern South American coast,
46 and suggest the Falkland Islands provide a valuable location for reconstructing high southern
47 latitude atmospheric circulation changes on multi-decadal to millennial timescales.

48

Zoe Thomas 11/10/2018 09:47

Deleted: modulating

Zoe Thomas 9/10/2018 16:21

Deleted: is of global importance in the Earth system

Zoe Thomas 11/10/2018 09:45

Deleted: (South Atlantic sector of the Southern Ocean)

Zoe Thomas 5/10/2018 15:18

Deleted: n

Zoe Thomas 5/10/2018 15:18

Deleted: area

Zoe Thomas 11/10/2018 09:35

Deleted: contemporary ASL dynamics

Zoe Thomas 11/10/2018 09:28

Deleted: and inconsistent with synoptic conditions associated with the ASL today

Zoe Thomas 11/10/2018 09:49

Deleted: across a large sector of the Southern Ocean

Zoe Thomas 9/10/2018 17:13

Deleted: The possible role of tropical Pacific in establishing contemporary-like synoptic circulation is explored.

64 **1. Introduction**

65 The leading mode of variability in atmospheric circulation across the southern mid-high
66 latitudes is the Southern Annular Mode (SAM), manifested as the pressure difference between
67 65°S and 40°S (Marshall, 2003; Thompson et al., 2011). The multi-decadal trend to a more
68 positive SAM since the mid-20th century (Fogt et al., 2012; Hosking et al., 2013) is expressed by
69 a strengthening and poleward shift of mid-latitude westerly airflow and storm tracks over the
70 Southern Ocean (Marshall, 2003; Thompson et al., 2011; Visbeck, 2009), and has been linked to
71 changes in climate, ocean ventilation, air-sea carbon flux, sea ice trends, and ice sheet dynamics
72 on interannual to multi-decadal timescales (Jones et al., 2016a; Landschützer et al., 2015;
73 Pritchard et al., 2012; Le Quéré et al., 2007; Thomas et al., 2018). Whilst the SAM may dominate
74 contemporary climate across the mid latitudes, other climate modes and atmospheric patterns
75 also play important roles both spatially and temporally. Arguably the most important in this
76 regard is the Amundsen Sea Low (ASL), a quasi-stationary low-pressure system located in the
77 Amundsen and Bellingshausen Seas (45-75°S, 180-60°W) - a consequence of the Antarctic
78 Peninsula and regional topography that dynamically influences atmospheric flow across this
79 sector of the Southern Ocean (Fogt et al., 2012; Hosking et al., 2013; Turner et al., 2013). Proxy
80 reconstructions of SAM and/or associated westerly winds have been generated for the Holocene
81 (Abram et al., 2014; Dixon et al., 2012; Fletcher and Moreno, 2012; Mayewski et al., 2017;
82 Moreno et al., 2012; Sime et al., 2010; Turney et al., 2017b) but there is a relative dearth of
83 records for the past behaviour of the ASL (Mayewski et al., 2013).

84
85 Seasonally, the ASL migrates across the Bellingshausen Sea into the Ross Sea: during the austral
86 summer, the pressure minimum extends east to the Antarctic Peninsula (reaching its lowest
87 geopotential height off coastal West Antarctica in the Amundsen Sea), while in winter, the ASL
88 migrates to the west into the eastern Ross Sea (Fogt et al., 2012). As a result, the ASL plays a
89 dominant role in climate and environmental variability across the wider south Pacific [and](#)
90 [southwestern South Atlantic](#) sectors of the Southern Ocean (Kreutz et al., 2000; Turner et al.,

91 | 2016). In particular, both the geopotential height and location of the ASL affects regional
92 | synoptic conditions that extend into the interior of West Antarctica and southern South America,
93 | (Clem et al., 2017; Ding et al., 2011; Schneider et al., 2012). Across the period 1979-2008
94 | (satellite era) the ASL appears to have deepened, with associated changes in the strength and
95 | location of the mid-latitude jet as described by the zonally-averaged SAM index (Jones et al.,
96 | 2016a). This deepening has been linked to stratospheric ozone depletion (Clem et al., 2017;
97 | Jones et al., 2016a; Raphael et al., 2016) as well as reduced sea ice along the western Antarctic
98 | Peninsula and climate changes across a broader sector of the Southern Ocean (Jones et al.,
99 | 2016a; Turner et al., 2013; Turney et al., 2016b). Other possible drivers of ASL dynamics
100 | operating on a range of timescales are changes in the equatorial Pacific (Abram et al., 2014;
101 | Ding et al., 2011; Lachlan-Cope and Connolley, 2006; Turney et al., 2017a) and the Interdecadal
102 | Pacific Oscillation (IPO) (Meehl et al., 2016); though these are not necessarily exclusive to one
103 | another.

Zoe Thomas 10/10/2018 15:46
Deleted: , modulated by changes in the tropical Pacific (Abram et al., 2014; Ding et al., 2011; Lachlan-Cope and Connolley, 2006; Turney et al., 2017a).
Zoe Thomas 9/10/2018 17:15
Deleted: ,

Zoe Thomas 10/10/2018 15:54
Deleted: with suggested links to
Zoe Thomas 11/10/2018 10:01
Deleted: more broadly with
Zoe Thomas 11/10/2018 10:01
Deleted: the
Zoe Thomas 10/10/2018 16:00
Deleted: southern Atlantic and Antarctic Peninsula

104 |
105 | The lack of long-term surface-based (*in situ*) observations in the Amundsen, Bellingshausen, and
106 | Ross Seas severely limits our understanding of the properties and impact of the ASL on multi-
107 | decadal to millennial timescales; an important consideration given uncertainties over the
108 | response of the ASL to future anthropogenic forcing (IPCC AR5, 2013). Fortunately,
109 | palaeoclimate proxy data from the region integrated with reanalysis data offers an opportunity
110 | to identify processes and mechanisms on timescales beyond those of satellite-era observations
111 | (since 1979). A major challenge for reconstructing changes in the ASL, however, is disentangling
112 | the role of mid-latitude westerly airflow associated with SAM. The location of the palaeo records
113 | and the proxies used are crucial in this regard. For instance, recent work from Siple Dome in
114 | West Antarctic recognised increased delivery of sea salt sodium (ssNa⁺) interpreted as
115 | representing a deepening of the ASL, with a particularly marked trend since 2900 years ago
116 | (hereafter 2.9 ka) (Mayewski et al., 2013). Although Siple Dome provides an important southern
117 | 'observation' point, information is needed on the northern side of the ASL to provide a more

128 complete reconstruction of its location and/or depth during the Holocene, as well a more
129 thorough understanding tropical Pacific-high latitude teleconnections. Here we report a new
130 high-resolution record of [local vegetation change and 'exotic' macrofossils – the latter a proxy](#)
131 [for westerly airflow](#) - extending the record over the past 5 ka and demonstrate a marked change
132 in synoptic conditions around 2.5 ka, providing important new insights into the long-term
133 behaviour of the ASL and the role of the tropic Pacific.

134

135 *1.1 Study site*

136 The Falkland Islands lie at 52°S, 540 km east of the coast of South America and 1500 km west of
137 subantarctic South Georgia. The present climate of the Falkland Islands is highly influenced by
138 the surrounding cool South Atlantic waters resulting in a cool temperate, maritime climate, with
139 corresponding low seasonality. Weather station data from the east Falkland Islands (Mount
140 Pleasant Airport) reveal a mean annual temperature of 5.5°C, high mean monthly and annual
141 wind speeds of ca. 8.5 m s⁻¹ (with prevailing westerly winds), and relatively low annual
142 precipitation of ca. 600 mm, distributed uniformly throughout the year (Lister and Jones, 2014).

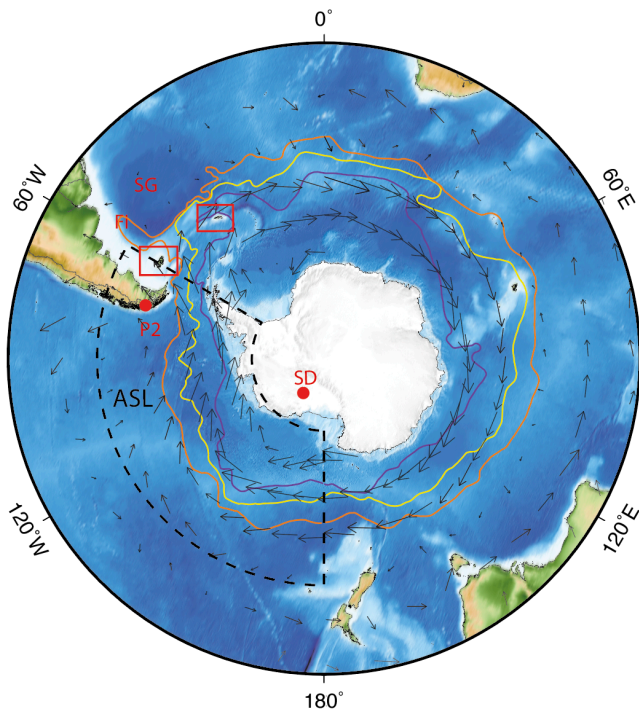
143

144 The Falkland Islands are dominated by extensive undulating lowlands, but several upland areas
145 in excess of 500 m above sea level (asl) occur within the archipelago. The islands are not
146 glaciated today and record only two periods of restricted glaciation in the Late Pleistocene
147 (Clapperton, 1971, 1990, 1993; Clapperton and Sugden, 1976; Roberts, 1984). Blanket peat was
148 established across large parts of the archipelago from 16.5 ka (Wilson et al., 2002). The islands
149 are situated within the main latitudinal belt of Southern Hemisphere westerly airflow (Barrow,
150 1978), and are therefore ideally placed to monitor changing Holocene wind strength across the
151 South Atlantic. The need to understand the climate impacts is an urgent one; recent studies have
152 suggested that with the projected increase in temperatures on the Falkland Islands, upland
153 species are highly vulnerable to climate change (Upson et al., 2016).

154

155 To investigate past airflow, a 1.5 m sequence was taken with a D-section corer from an exposed
156 Ericaceous-grass peatland on Canopus Hill (51.691°S, 57.785°W, approximately 30 m asl),
157 outside Port Stanley (35 km from Mount Pleasant Airport). The uniform dark-brown peat was
158 contiguously sampled for pollen, charcoal and comprehensive radiocarbon dating. Work at this
159 site has previously recognised the input of exotic pollen and charcoal derived from South
160 America but was limited to the last 2.5 kyr (Turney et al., 2016a),

Zoe Thomas 8/10/2018 10:43
Deleted: , with changes to westerly airflow
over the past ~2.5 ka



162 **Figure 1.** Location of the Falkland Islands (FI), South Georgia [SG], Siple Dome [SD] and Palm 2
163 [P2]. Dashed line denotes contemporary limits of the ASL domain defined across the 1979–2001
164 average (Fogt et al., 2012). Mean locations of the southern limb of the Antarctic Circumpolar
165 Current (purple), the polar front (red) and the subantarctic front (green) are shown, following
166 Orsi et al. (1995), based on analyses of hydrographic station data available up to 1990. The grey
167 arrows denote the 925 hPa winds (vectors) trends since 1979 from ERA-Interim (Dee et al.,

170 | [2011](#)), depicting the location and increase in westerly winds over the satellite era. Map made
171 | [using Generic Mapping Tools \(GMT\)](#) (Wessel et al., 2013).

172

173 | **2. Methods**

174

175 | **2.1 Pollen *and charcoal* analysis**

176 | The pollen samples were prepared using standard palynological techniques (Faegri and Iverson,
177 | 1975). Volumetric samples were taken every 1 cm along the core, with *Lycopodium* spores
178 | added as a 'spike'. The samples were deflocculated with hot 10% NaOH and then sieved through
179 | a 106 µm mesh, before acetolysis, to remove extraneous organic matter. The samples were
180 | mounted in silicon oil and pollen types/palynomorphs were counted at 400× magnification
181 | until a minimum of 300 target grains were identified. Pollen/palynomorphs were identified
182 | using standard pollen keys (Barrow, 1978; Macphail and Cantrill, 2006) and the pollen type
183 | slide collection at the University of Exeter, UK. The pollen counts were expressed as
184 | percentages, with only total land pollen (TLP) contributing to the final pollen sum. The
185 | *Lycopodium* 'spike' was also used to calculate total and individual pollen concentrations (grains
186 | cm⁻³) (Stockmarr 1971), and these values were divided by the deposition time (year cm⁻¹) to
187 | calculate pollen accumulation rates (PAR; grains cm⁻² year⁻¹). Major pollen zone boundaries
188 | were determined using CONISS (stratigraphically constrained cluster analysis) (Grimm, 1987)
189 | using the rioja package in R (Juggins, 2017). Past fire activity was investigated using counts of
190 | micro-charcoal fragments (< 106 µm) identified on the pollen slides (Whitlock and Larsen,
191 | 2001). Counts were undertaken at each level until a fixed total of 20 *Lycopodium* spores were
192 | counted and the total expressed as a concentration (fragments per cm³). Charcoal accumulation
193 | rate (CHAR) was calculated by dividing the total charcoal concentration by the deposition time
194 | estimated from the age-depth relationship.

195

196

Zoe Thomas 5/10/2018 15:05

Deleted: Figure 1. Location of the Falkland Islands (FI), South Georgia [SG], Siple Dome [SD] and Palm2 [P2]. Dashed line denotes contemporary defined limits of the ASL domain (Fogt et al., 2012). Location of the polar front (yellow line) and direction of the Southern Hemisphere westerly winds (black arrows) are also shown. Map made using Generic Mapping Tools (GMT) (Wessel et al., 2013).

Page Break

Zoe Thomas 9/10/2018 16:57

Deleted: -

... [1]

211 | 2.2 Radiocarbon and ¹³⁷Cs dating

212 | To derive a chronological framework for the Canopus Hill peat sequence, terrestrial plant
213 | macrofossils (fruits and leaves) were extracted. These macrofossils were given an acid–base–
214 | acid (ABA) pre-treatment and then combusted and graphitised in the University of Waikato
215 | AMS laboratory, with ¹⁴C/¹²C measurement by the University of California at Irvine (UCI) on a
216 | NEC compact (1.5SDH) AMS system. The pre-treated samples were converted to CO₂ by
217 | combustion in sealed pre-baked quartz tubes, containing Cu and Ag wire. The CO₂ was then
218 | converted to graphite using H₂ and an Fe catalyst, and loaded into aluminium target holders for
219 | measurement at UCI. The ¹⁴C measurements were supplemented by ¹³⁷Cs measurements near
220 | the top of the profile to detect the onset of nuclear tests in the mid-20th century. The
221 | anthropogenic radionuclide ¹³⁷Cs (with a half time of 30 years) is derived from atmospheric
222 | nuclear weapons testing and can provide an important “first appearance” horizon of known age
223 | (1954–1955) i.e. an independent marker horizon to assist with age model validation (Hancock
224 | et al., 2011). ¹³⁷Cs analysis was undertaken following standard techniques with measurements
225 | made using an ORTEC high-resolution, low-background coaxial germanium detector.
226 | Specifically, we analysed contiguous peat samples for the first presence of ¹³⁷Cs; detectable
227 | measurements were obtained down to 8.5-9.5 cm.

Zoe Thomas 9/10/2018 16:57

Deleted: 3

228 |
229 | 2.3 Age modelling

230 | The ¹⁴C and ¹³⁷Cs ages were used to develop an age model using a P_{sequence} deposition model
231 | in OxCal 4.2 (Bronk Ramsey, 2008; Bronk Ramsey and Lee, 2013); with the General Outlier
232 | analysis detection method (probability=0.05) (Bronk Ramsey, 2009). The ¹⁴C ages were
233 | calibrated against the Southern Hemisphere calibration (SHCal13) data set (Hogg et al., 2013).
234 | The model was based on 1000 iterations, with the surface (depth zero) and year of sampling
235 | (2010) as the uppermost chronological control point. Using Bayes' theorem, the algorithms
236 | employed sample possible solutions with a probability that is the product of the prior and
237 | likelihood probabilities (Bronk Ramsey, 2008). Taking into account the deposition model and

Zoe Thomas 9/10/2018 16:57

Deleted: 4

Zoe Thomas 5/10/2018 15:26

Deleted: The two basal ages were found in ;
two were excluded due to an age inversion,
possibly a result of root penetration.

243 the actual age measurements, the posterior probability densities quantify the most likely age
 244 distributions; the outlier option was used to detect ages that fall outside the calibration model
 245 for each group, and if necessary, down-weight their contribution to the final age estimates. The
 246 first presence of ¹³⁷Cs was assigned the prior U(1952, 2011) in the OxCal age model to capture
 247 the possible range of calendar years (CE) for the onset of ¹³⁷Cs deposition in the sequence
 248 (Hancock et al., 2011). Modelled ages are reported here as thousands of calendar years before
 249 present (CE 1950) or ka (Table 1). We used the mean of the modelled age solutions to estimate
 250 the age of a fraction at each sample depth. The radiocarbon ages follow a stratigraphic order
 251 except for the two basal ages. We suspect these basal ages may comprise intruded younger root
 252 material; a scenario not unusual in relatively slowly accumulating sedimentary sequences e.g.
 253 (Brock et al., 2011). The sedimentation rate is internally more consistent when excluding these
 254 two basal ages; without them the sedimentation rate from the entire metre of sediment above
 255 does not change significantly (with a sedimentation rate for 141.5-156 cm of 38 yrs/cm
 256 compared to an average of 27 yrs/cm for the preceding metre of sediment), whereas including
 257 them increases the sedimentation rate over this depth range abruptly to 11.6 yrs/cm. The
 258 calibrated 2σ age range for both the age model including and excluding these two basal ages are
 259 found in Table 1; the calibrated age ranges are almost identical for both age models until 142
 260 cm, from where it diverges. Importantly, our conclusions are not at all affected by the choice of
 261 age model.

Zoe Thomas 11/10/2018 10:12
Deleted:
 Zoe Thomas 10/10/2018 16:51
Deleted: and Figure 2
 Zoe Thomas 11/10/2018 10:13
Deleted: The multi-proxy sequence reported here spans the last 5 ka (Figure 2).

Depth, cm	Wk lab number	Material	% Modern / ¹⁴ C BP ± 1 σ	2σ cal. age range	2σ cal. age range	Mean cal. age (years BP)
				(years BP)	(years BP)	
				With 2 basal ages	Excluding 2 basal ages	
8-9	34598	Fruits and leaves	117.0±0.4%M	-4 to -43	-4 to -44	-21
9		¹³⁷ Cs		-6 to -42	-6 to -42	-19
11-12	32994	Fruits and leaves	107.8±0.4%M	-2 to -14	-1 to -14	-8
18-19	37007	Fruits and leaves	107.3±0.3%M	0 to -13	26 to -15	-3
25-26	35146	Fruits and leaves	95±25	250 to -1	250 to -1	86
35-36	37008	Fruits and leaves	650±25	650 to 550	650 to 550	600
39-40	33445	Fruits and leaves	760±25	720 to 570	720-570	660
57-58	32996	Fruits and leaves	1820±25	1800 to 1600	1800 to 1600	1680
70-71	32350	Fruits and leaves	2240±25	2320 to 2100	2310 to 2100	2220

97-98	32997	Fruits and leaves	2750±25	2870 to 2760	2870 to 2760	2810
107-108	32998	Fruits and leaves	2910±26	3140 to 2880	3140 to 2880	3000
120-121	41767	Fruits and leaves	3240±20	3480 to 3360	3470 to 3360	3420
141-142	32351	Fruits and leaves	3960±32	4430 to 4180	4510 to 4240	4350
148-149	41768	Fruits and leaves	4390±20	4520 to 4300	5030 to 4850	4910
153.5-154.5	42144	Fruits and leaves	4040±21	4520 to 4420		
156.5-157.5	42145	Fruits and leaves	4080±22	4570 to 4430		

267
268 **Table 1.** Radiocarbon and modelled calibrated age ranges for the Canopus Hill peat sequences
269 using the P_sequence and Outlier analysis option in OxCal 4.2 (Bronk Ramsey, 2008; Bronk
270 Ramsey and Lee, 2013). The SHCal13 (Hogg et al., 2013) and Bomb04SH (Hua and Barbetti,
271 2004) calibration curves were used. Note: calibrated ages are relative to Before Present (BP) i.e.
272 CE 1950.

273

274

275 3. Results and Discussion

276

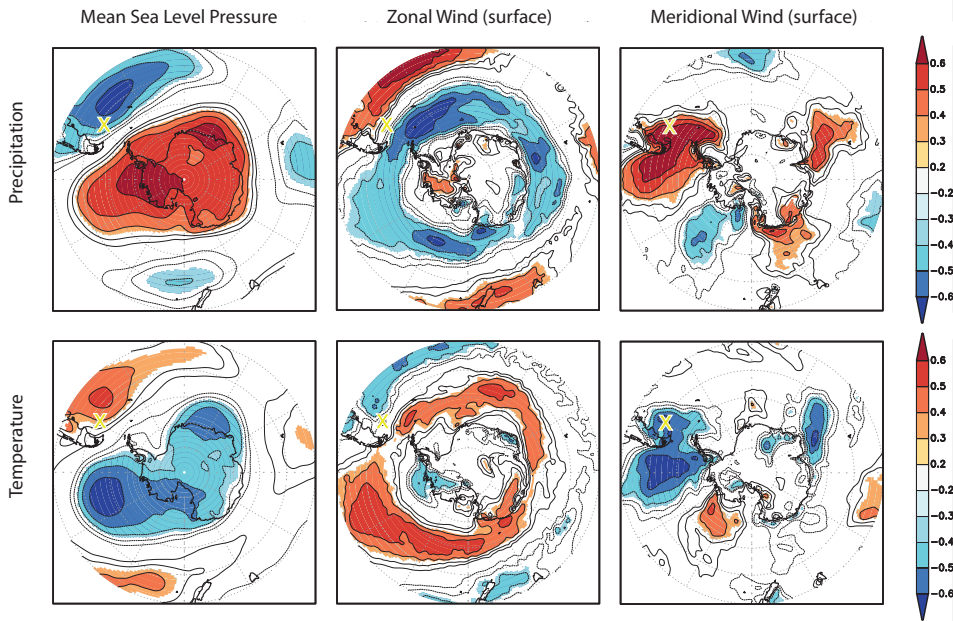
277 3.1 Contemporary Climate

278 Regional climate dynamics were explored using the ERA Interim reanalysis (Dee et al., 2011),
279 and the instrumental observations from Mount Pleasant Airport weather station on the
280 Falkland Islands (Jones et al., 2016b; Lister and Jones, 2014). Given the seasonal nature of
281 vegetation growth (including peat accumulation), spatial correlations using deseasonalised and
282 detrended (to remove potential bias as a result of similar seasonal and long-term trends)
283 spring-summer precipitation and temperature were investigated. These analyses show
284 important links with atmospheric synoptic conditions (Figure 2) including a clear link between
285 precipitation and zonal and meridional circulation (Figure 2c). Spatial correlations suggest
286 limited ocean influence on these climate variables on the Falkland Islands. Crucially, wetter
287 conditions are associated with a weakening of the ASL and the delivery of more southerly and
288 easterly airflow across the South Atlantic (Jones et al., 2016b). Conversely, more northerly
289 airflow is associated with less precipitation over the Falklands. A similar picture emerges with

290 variations in temperature (Figure 2a and d) with a deeper (i.e. more intense low pressure) ASL
291 associated with warmer temperatures over the Falkland Islands, and a weaker ASL with cooler
292 conditions.

293

294



295

296

297 **Figure 2.** Spatial correlation of relationships between precipitation, temperature and synoptic
298 conditions from Mount Pleasant Airport (October to March), Falkland Islands ('X'). Mean Sea
299 Level Pressure (MSLP), surface zonal wind and surface meridional wind correlated with
300 October to March precipitation (upper row) and temperature (lower row) using ERA-79 Interim
301 reanalysis (Dee et al., 2011) (1979–2013). Significance $p_{field} < 0.05$. Analyses were made with
302 KNMI Climate Explorer (van Oldenborgh and Burgers, 2005).

303 3.2 Holocene Climate and Environmental Change

304 The Canopus Hill peat sequence reported here from the Falkland Islands represents one of the
305 longest pollen records from the South Atlantic, with the only published early Holocene record
306 from Barrow et al. (1978), which has limited age control and resolution. Our reconstruction
307 appears to represent changing environmental conditions through the mid to late Holocene
308 (Figure 3). The pollen record is dominated by Poaceae and *Empetrum*, consistent with both
309 previous studies and current vegetation on the islands (Barrow, 1978; Broughton and Mcadam,
310 2003; Clark et al., 1998; Turney et al., 2016a). However, in contrast to these previous studies,
311 we observe a major shift in the representation of Cyperaceae and the total accumulation of
312 pollen centred on ~2.5 ka (Figure 4).

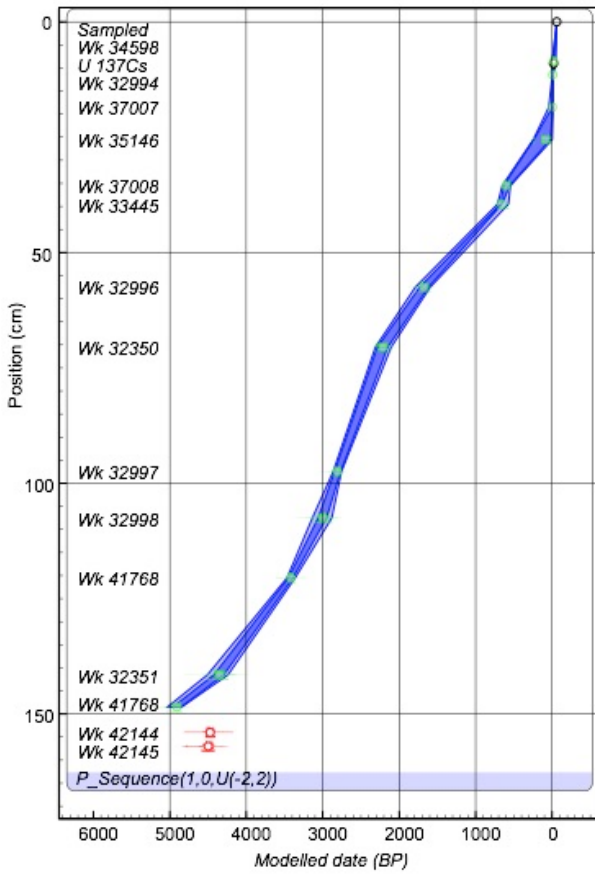
Zoe Thomas 30/9/2018 12:45
Deleted: (Barrow, 1978; Turney et al., 2016a)

Zoe Thomas 9/10/2018 16:46
Deleted: through the mid- to late-Holocene

Zoe Thomas 10/10/2018 16:27
Deleted: 3

313
314 Similar changes to the above are also observed in the aeolian transportation of exotic pollen and
315 charcoal derived from long-distance transport. These 'exotic' pollen in the Canopus Hill
316 sequence represent South American flora delivered to the site by westerly airflow. While only
317 representing between 0.3% and 4.6% of the pollen sum, we recorded *Nothofagus*, *Podocarpus*,
318 *Ephedra fragilis*, and *Anacardium*-type (arboreal) pollen grains. *Nothofagus* was the most
319 frequently recorded exotic taxon in the samples, due to its high representation on Tierra del
320 Fuego and the Islas de los Estados (upstream of the Falkland Islands), and high production of
321 wind-dispersed pollen that can be carried over long distances (Moreno et al., 2009). In extreme
322 situations, *Nothofagus* pollen has been recovered as far from South America as Marion Island
323 and Tristan da Cunha (Hafsten, 1960; Mildenhall, 1976; Wace and Dickson, 1965).

324

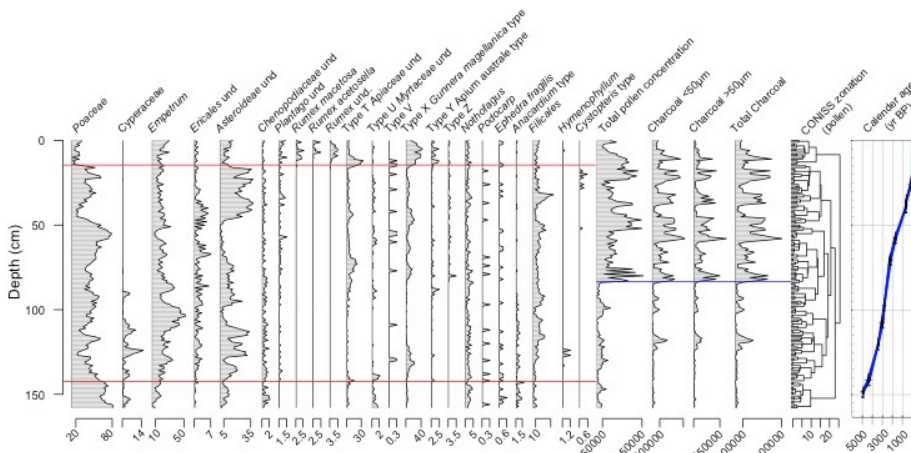


330

331

332 Figure 3. The age-depth relationship from Canopus Hill, with 1σ and 2σ age range (dark and
 333 light blue envelopes respectively) and probability distributions generated from the Bayesian
 334 age model. Red symbols indicate radiocarbon ages not incorporated into the age model.
 335 Calibrated using SHCal13 atmospheric curve (Hogg et al., 2013) and 'Post-bomb' atmospheric
 336 SH curve (Hua and Barbetti, 2004). Plot made with OxCal v4.3.2 (Bronk Ramsey, 2017).

337



338

339 **Figure 4:** Summary pollen diagram from Canopus Hill, Port Stanley, with the left hand panels
 340 describing palynomorphs as percentages of the total land pollen plotted against depth. The
 341 middle panels show total pollen, charcoal of different size fractions and total charcoal expressed
 342 as a concentration (number cm^{-3}). Parallel lines denote major pollen (red) and charcoal/pollen
 343 concentration (blue) zone boundaries were determined using CONISS (Grimm, 1987).

344

345

346

Zoe Thomas 10/10/2018 17:26
 Deleted: <sp>

Zoe Thomas 10/10/2018 16:23
 Deleted: 3

Zoe Thomas 10/10/2018 16:21
 Moved down [2]: The far right panel depicts the age-depth relationship, with 1σ age range (blue envelope) and probability distributions generated from the Bayesian age model.

Zoe Thomas 10/10/2018 16:21
 Moved (insertion) [2]

Zoe Thomas 10/10/2018 16:22
 Deleted: The far right panel depicts the age-depth relationship, with 1σ age range (blue envelope) and probability distributions generated from the Bayesian age model.

359 Differences in the exotic pollen assemblages can reflect either changes in the transport pathway
360 (i.e. direction and wind strength) or regional vegetation change in the source area(s). Today,
361 *Nothofagus* dominates lowland Patagonian vegetation and is found throughout Patagonian Late
362 Glacial sequences. This taxa is thought to have been most widely established by 5 ka (Iglesias et
363 al., 2014; Kilian and Lamy, 2012), with a reasonably constant representation until stepped
364 expansion at Lago Guanaco, almost directly west of the Falklands (51.03°S, 72.83°W, 185m asl),
365 centred on 570 cal. years (Moreno et al., 2009; Villa-martínez et al., 2012). Fire activity and the
366 introduction of exotic weeds introduced by European settlers is thought to have resulted in the
367 rapid decline of *Nothofagus* at the end of the 19th century (Moreno et al., 2009). The fact that
368 *Nothofagus* is consistently represented throughout the Canopus Hill record indicates pervasive
369 westerly winds throughout the mid to late-Holocene, but does not have sufficiently high
370 concentrations to robustly identify long-term changes.

371

372 Recent syntheses of charcoal stratigraphies across Patagonia have detected regional trends in
373 biomass burning during the Holocene with a moderate increase occurring over the last 3000
374 years (Huber et al., 2004; Whitlock et al., 2007; Power et al., 2008). Highly variable counts of
375 charcoal were obtained through the Canopus Hill sequence, however, more than 99% of
376 charcoal fragments were less than 50 µm in size, with negligible amounts identified in the 50–
377 106 µm and >106 µm fractions (Figure 4). As charcoal of this size can be transported long
378 distances (Clark, 1988) it is likely that this influx of charcoal predominantly represent South
379 American sources and westerly (and south-westerly) airflow, and that there was little or no fire
380 in the local environment throughout the mid- to late-Holocene. The presence of fire in the
381 Patagonian landscape during the late Holocene thus provides a ready source of exotic material
382 for aerial transport to the Falkland Islands delivered via westerly airflow. The aeolian delivery
383 of the charcoal to the Falkland Islands is supported by a correspondence between the Canopus
384 Hill and Lago Guanaco, Southwest Patagonia (Moreno et al., 2009) charcoal records. There is

Zoe Thomas 8/10/2018 11:25

Moved (insertion) [1]

Zoe Thomas 10/10/2018 16:23

Deleted: 3

Zoe Thomas 30/9/2018 09:54

Deleted: ,

Zoe Thomas 8/10/2018 11:24

Deleted: the close

388 also a weak correlation between charcoal and *Nothofagus*, particularly in the younger half of the
389 record, probably reflecting the similar transport modes.

391 Centennial-scale variability in the Canopus Hill charcoal record over the last 2.5 kyr has
392 previously been identified, apparently coherent with radiocarbon production rates (Turney et
393 al., 2016a), suggesting that solar variability has a modulating influence on Southern Hemisphere
394 westerly airflow. Similar cyclical variations in West Antarctic Peninsula glacier discharge as
395 observed from the $\delta^{18}\text{O}_{\text{diatom}}$ record from Site 1099 in the Palmer Deep, has also been reported
396 (Pike et al., 2013) which shows an underlying decrease towards lower values, reported from
397 ~2.5 kyr. Specifically, this increased glacial ice discharge is considered to have been driven by
398 atmospheric warming (as a result of peak local summer insolation; Figure 5), supporting the
399 findings from Canopus Hill.

401 3.3 Holocene changes in the Amundsen Sea Low (ASL)

402 Our results support the notion of pervasive westerly winds throughout the mid- to late-
403 Holocene, as shown by the consistent representation of *Nothofagus* pollen, as well as the pollen
404 of other rare exotic taxa including *Podocarp*, *Ephedra fragilis* and *Anacardium*-type found
405 throughout the Canopus Hill peat sequence. Whilst the presence of *Nothofagus* implies westerly
406 airflow has been maintained across the South Atlantic, the relatively high expression of
407 Cyperaceae between 5 and ~2.5 ka (Figure 5) suggests enhanced delivery of cooler and moister
408 air to the Falklands. Our analyses exploring contemporary drivers of synoptic conditions imply
409 these conditions could have been brought about by more southerly airflow across the South
410 Atlantic (Figure 2), synoptic conditions inconsistent with today's expression of the ASL. The
411 marked decline in Cyperaceae and increase in charcoal at ~2.5 ka indicates a shift to drier and
412 potentially warmer conditions, most probably a result of reduced southerly airflow and the
413 northward movement and/or expansion of the ASL. The inferred increase in primary

Zoe Thomas 8/10/2018 11:25

Moved up [1]: Recent syntheses of charcoal stratigraphies across Patagonia have detected regional trends in biomass burning during the Holocene with a moderate increase occurring over the last 3000 years (Huber et al., 2004; Whitlock et al., 2007; Power et al., 2008).

Zoe Thomas 10/10/2018 16:24

Deleted: 4

422 productivity and pollen accumulation on the islands supports this interpretation (Turney et al.,
423 2016b).

424

425 These results complement other studies from the broader South Atlantic region (Figure 5). Ice
426 core-derived proxies from Siple Dome, located in a key region for understanding ASL dynamics,
427 imply distinct changes in atmospheric circulation. Here, $ssNa^+$ provides a measure of sea-salt
428 species, the transport of which is significantly influenced by the ASL (Kreutz et al., 2000), with

429 higher values associated with a deeper ASL. The long-term increase of $ssNa^+$ over the mid- to
430 late Holocene, thus implies a deepening of the ASL (Mayewski et al., 2013) consistent with our

431 data. The slight difference in the timing between these records may be a consequence of
432 chronological uncertainties or a lag in the projection of the ASL onto the South Atlantic (possibly
433 reflecting an eastward migration/extension of the ASL to where it is more commonly located

434 today). Farther north, the marine sequence from the Palm2 within the Skyring fjord system
435 west of the Andean crest of South America shows strong fluctuations of biogenic carbonate

436 accumulation rates in superficial fjord waters (Lamy et al., 2010). This record represents
437 marine carbonate production and its subsequent accumulation on the sea bed in response to
438 salinity changes in the upper water column of the fjord; prevailing westerly winds keep the low-

439 salinity waters inside the fjord, therefore, lower salinity anomalies suggest stronger westerly
440 winds. Intriguingly, the Palm2 record shows a pronounced sustained decrease in salinity

441 anomalies from ~2/2.5 ka (Figure 5), interpreted to be a result of a strengthening of mid-
442 latitude westerly winds and possible influence of the ASL, consistent with our reconstruction.

443 The differences in the timing within the records that we compare may be an artefact of the
444 uncertainties in the individual age models, or represent real dynamic changes operating on

445 multi-decadal to centennial timescales. The changes at Palm2 do appear to be more abrupt than
446 those observed from Siple Dome, but we do not interpret this as a regime shift (Thomas, 2016).

447 The last age control point for the Palm2 record is from a marine shell at the start of the
448 inflection, dating to 2570 ± 30 ^{14}C BP, calibrated to 2410 cal yr BP (no 2σ age range given),

Zoe Thomas 30/9/2018 13:02

Deleted: i

Zoe Thomas 10/10/2018 16:24

Deleted: 4

Zoe Thomas 8/10/2018 10:18

Deleted: (~2.9 ka)

Zoe Thomas 9/10/2018 14:10

Deleted: PALM2

Zoe Thomas 11/10/2018 10:22

Deleted: e

Zoe Thomas 11/10/2018 10:23

Deleted: a

Zoe Thomas 9/10/2018 13:33

Deleted: Carbonate preservation in this record is interpreted to be a proxy for salinity changes as a result of

Zoe Thomas 9/10/2018 13:33

Deleted: that

Zoe Thomas 9/10/2018 13:45

Deleted: ;

Zoe Thomas 9/10/2018 13:45

Deleted: therefore

Zoe Thomas 9/10/2018 14:10

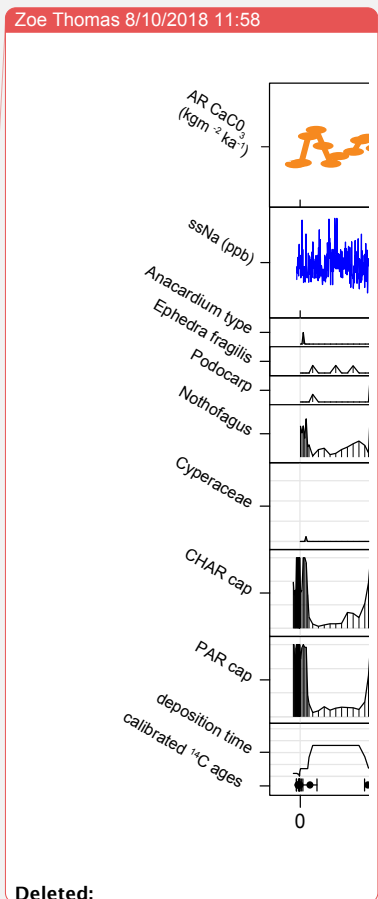
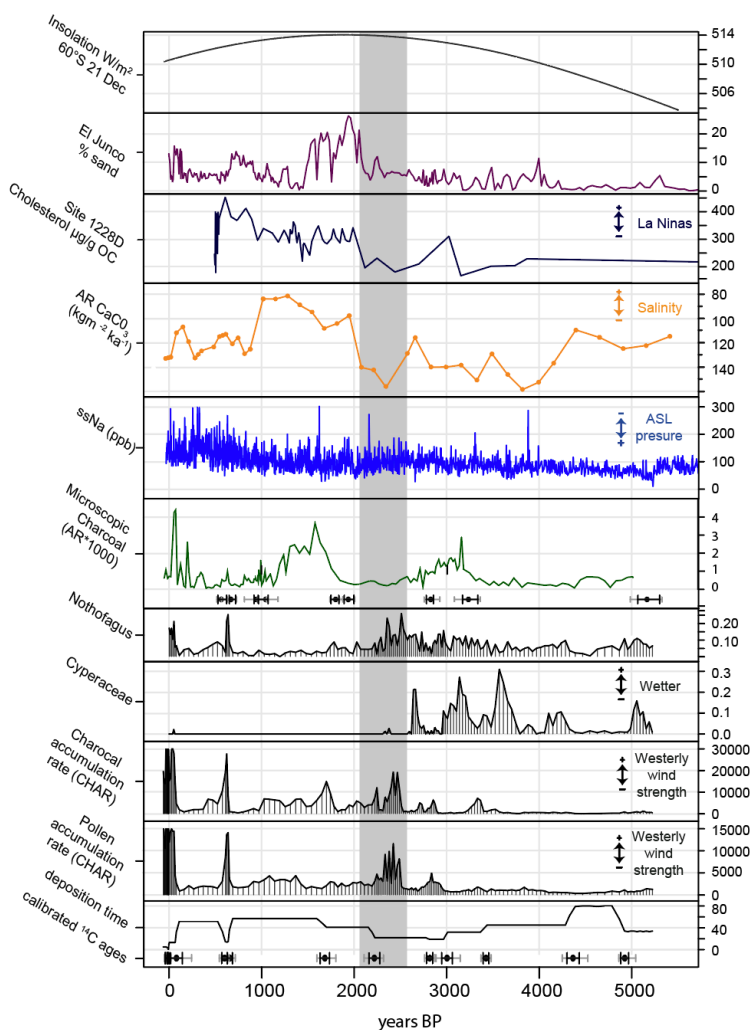
Deleted: PALM2

462 [suggesting the age uncertainties between the changes observed in the Canopus Hill record and](#)
463 [the Palm2 record may possibly overlap.](#)

464

465 Taken together the above results imply that there was a long-term change in the behaviour of
466 the ASL with the establishment of contemporary synoptic conditions around 2.5 ka. The reason
467 for a change at ~2.5 ka is not immediately apparent but one possibility is the tropical Pacific.
468 Today, equatorial Pacific ocean-atmospheric linkages are known to modulate the ASL with
469 associated impacts across the broader region including climate, sea ice and ice sheet dynamics
470 (Abram et al., 2014; Ding et al., 2011; Lachlan-Cope and Connolley, 2006; Turney et al., 2017a).
471 Reconstructions of sea surface temperatures and precipitation suggest the establishment of
472 more pervasive El Niño-Southern Oscillation (ENSO) activity from 3 to 2.5 ka (Carre et al., 2014;
473 Makou et al., 2010; Rein et al., 2005), that may have been projected onto the southeast Pacific
474 sector of the Southern Ocean (Abram et al., 2014). [The ENSO circulation pattern is](#)
475 [teleconnected to Southern Ocean and Antarctic climate, in particular the Amundsen Sea low-](#)
476 [pressure region, possibly via movements of the South Pacific Convergence Zone](#) (Russell and
477 [McGregor, 2010\). Contemporary La Niña events are accompanied by a northerly shift in the](#)
478 [South Pacific Convergence Zone and the production of cyclones in the region of the Amundsen](#)
479 [Sea low, enhancing warm northerly airflow over Patagonia, the Western Antarctic Peninsula](#)
480 [and the Falkland Islands. In addition, Fogt et al. \(2011\) found that when a La Niña event occurs](#)
481 [during a positive phase of the SAM, the ASL deepens, suggesting that the SAM and the ASL may](#)
482 [modulate one another. Whilst a shift to more negative IPO has been linked to a deepening of the](#)
483 [ASL](#) (Meehl et al., 2016), [the long-term changes in this climate mode are currently uncertain.](#)
484 Given the projected increase in extreme ENSO events under future anthropogenic forcing (Cai et
485 al., 2015) further work is needed to determine the mechanisms, timing and impacts of these low
486 to high latitude teleconnections through the Holocene.

487



488

489 Figure 5: Key data from the Canopus Hill sequence (Falkland Islands) and other South Atlantic
 490 records. From bottom to top: deposition time, total pollen accumulation rate (PAR), total
 491 charcoal accumulation rate (CHAR), Cyperaceae and Nothofagus re-expressed as accumulation
 492 rates, microscopic charcoal from Lago Guanaco (Moreno et al. 2009), ssNa+ from Siple Dome
 493 (Mayewski et al., 2013), salinity anomalies from Palm2 (Lamy et al., 2010), cholesterol
 494 abundance, ODP Site 1228, Peru margin (Makou et al., 2010), percentage of sand, El Junco
 495 Crater Lake, Galápagos (Conroy et al., 2008) and summer (21 Dec) insolation (W/m²) at 60°S

497 (Laskar et al., 2004). Calibrated radiocarbon ages and 1σ (black) and 2σ (grey) age ranges for
498 Canopus Hill and Lago Guanaco are plotted at the base of the respective panel. Note that PAR
499 and CHAR have both been truncated at the modern end due to high accumulation rate. The grey
500 boxed area marks the transition period during which the ASL strengthened over the South
501 Atlantic.

502

503

504 4. Conclusion

505

506 The Amundsen Sea Low (ASL) has been recognized as an important driver of Southern Ocean
507 climate and environmental changes during the late twentieth century. Unfortunately, however,

508 there are limited observational and proxy datasets capturing the long-term behaviour and

509 impact of the ASL. Here we report a comprehensively dated peat record from Canopus Hill

510 (Falkland Islands) in the southwestern South Atlantic Ocean, a region highly sensitive to the

511 ASL. Our multi-proxy study including local vegetation change and exotic pollen and charcoal

512 (wind-blown macrofossils originating from South America) allows us to reconstruct climate

513 changes over the last 5000 years. We observe a marked shift from pervasive wet and cool to

514 drier and warmer conditions around 2500 years ago. ERA Interim reanalysis suggests this

515 change was a consequence of the establishment of contemporary westerly airflow associated

516 with the ASL projecting onto the South Atlantic. The timing of this change is consistent with

517 increased surface warming and expression of the El Niño-Southern Oscillation (ENSO) in the

518 region, suggesting a strengthening of equatorial-high latitude atmospheric teleconnections. Our

519 study demonstrates the value of the Falkland Islands for reconstructing atmospheric circulation

520 changes across the southwestern South Atlantic on multi-decadal to millennial timescales.

521

522

523

Zoe Thomas 8/10/2018 11:59

Deleted: Figure 4: Key data from the Canopus Hill sequence (Falkland Islands) and other South Atlantic records. From bottom to top: deposition time, total pollen accumulation rate (PAR), total charcoal accumulation rate (CHAR), *Cyperaceae*, *Nothofagus*, *Podocarp*, *Ephedra*, *Anacardium*-type re-expressed as accumulation rates, ssNa⁺ from Siple Dome (Mayewski et al., 2013) and salinity anomalies from PALM2 (Lamy et al., 2010). Calibrated radiocarbon ages and 1σ range are plotted at the base of the figure. Note that PAR and CHAR have both been capped at the modern end due to high accumulation rate. The grey boxed area marks the period during which there was limited expression of the ASL over the South Atlantic.

Zoe Thomas 11/10/2018 10:31

Deleted: Whilst the Southern Annular Mode (SAM) dominates climate variability in the mid-latitudes of the Southern Hemisphere, other climate modes and atmospheric patterns

Zoe Thomas 11/10/2018 10:32

Deleted: play

Zoe Thomas 11/10/2018 10:32

Deleted: important role

Zoe Thomas 11/10/2018 10:31

Deleted: s, some of which are of global significance

Zoe Thomas 9/10/2018 16:52

Deleted: One of the most important is the atmospheric pressure centre known as the Amundsen Sea Low (ASL).

Zoe Thomas 9/10/2018 16:55

Deleted:

Zoe Thomas 9/10/2018 16:53

Deleted: including

Zoe Thomas 9/10/2018 16:53

Deleted: exotic

Zoe Thomas 9/10/2018 16:55

Deleted: taxa

Zoe Thomas 9/10/2018 16:55

Deleted: and charcoal

Zoe Thomas 9/10/2018 16:58

Deleted: a large sector of the Southern Ocean

561 **Acknowledgements**

562 We would like to acknowledge the incredible debt we owe to our close friend and colleague
563 Richard Jones without whom this work would not have been possible. We miss you Richard.
564 This project was supported by the Australian Research Council (FL100100195 and
565 DP130104156). We thank the Falkland Islands Government for permission to undertake
566 sampling on the island (permit number R07/2011) and Darren Christie for assisting with the
567 fieldwork.

568

569

570 **References**

571 Abram, N. J., Mulvaney, R., Vimeux, F., Phipps, S. J., Turner, J. and England, M. H.: Evolution of the
572 Southern Annular Mode during the past millennium, *Nat. Clim. Chang.*, 4(7), 1–6,
573 doi:10.1038/NCLIMATE2235, 2014.

574 Barrow, C.: Postglacial pollen diagrams from south Georgia (sub-Antarctic) and West Falkland
575 island (South Atlantic), *J. Biogeogr.*, 5(3), 251–274, doi:10.2307/3038040, 1978.

576 Brock, F., Lee, S., Housley, R. A. and Bronk Ramsey, C.: Variation in the radiocarbon age of
577 different fractions of peat: A case study from Ahrenshöft, northern Germany, *Quat. Geochronol.*,
578 6(6), 550–555, doi:10.1016/j.quageo.2011.08.003, 2011.

579 Bronk Ramsey, C.: Deposition models for chronological records, *Quat. Sci. Rev.*, 27(1–2), 42–60,
580 doi:10.1016/j.quascirev.2007.01.019, 2008.

581 Bronk Ramsey, C.: Dealing with outliers and offsets in radiocarbon dating, *Radiocarbon*, 51(3),
582 1023–1045, 2009.

583 Bronk Ramsey, C. and Lee, S.: Recent and Planned Developments of the Program OxCal,
584 *Radiocarbon*, 55(2–3), 720–730, doi:10.2458/azu_js_rc.55.16215, 2013.

585 Broughton, D. A. and Mcadam, J. H.: The current status and distribution of the Falkland Islands
586 pteridophyte flora, *Fern Gaz.*, 17(1), 21–38, 2003.

587 Cai, W., Santoso, A., Wang, G., Yeh, S., An, S., Cobb, K. M., Collins, M., Guilyardi, E., Jin, F., Kug, J.,

588 Lengaigne, M. and McPhaden, M. J.: ENSO and greenhouse warming, *Nat. Clim. Chang.*, 5(9), 849–
589 859, doi:10.1038/nclimate2743, 2015.

590 Carre, M., Sachs, J. P., Purca, S., Schauer, A. J., Braconnot, P., Angeles Falcon, R., Julien, M. and
591 Lavallee, D.: Holocene history of ENSO variance and asymmetry in the eastern tropical Pacific,
592 *Science*, 345(6200), 1045–1048, 2014.

593 Clark, J. S.: Particle Motion and the Theory of Charcoal Analysis: Source Area, Transport,
594 Deposition, and Sampling, *Quat. Res.*, 30, 67–80, 1988.

595 Clark, R., Huber, U. M. and Wilson, P.: Late Pleistocene sediments and environmental change at
596 Plaza Creek, Falkland Islands, South Atlantic, *J. Quat. Sci.*, 13(2), 95–105,
597 doi:10.1002/(SICI)1099-1417(199803/04)13:2<95::AID-JQS351>3.0.CO;2-G, 1998.

598 Clem, K. R., Renwick, J. A. and McGregor, J.: Large-Scale Forcing of the Amundsen Sea Low and Its
599 Influence on Sea Ice and West Antarctic Temperature, *J. Clim.*, 30, 8405–8424,
600 doi:10.1175/JCLI-D-16-0891.1, 2017.

601 Conroy, J. L., Overpeck, J. T., Cole, J. E., Shanahan, T. M. and Steinitz-Kannan, M.: Holocene
602 changes in eastern tropical Pacific climate inferred from a Galápagos lake sediment record,
603 *Quat. Sci. Rev.*, 27(11–12), 1166–1180, doi:10.1016/j.quascirev.2008.02.015, 2008.

604 Dee, D. P., Uppala, S. M., Simmons, A. J., Berrisford, P., Poli, P., Kobayashi, S., Andrae, U.,
605 Balmaseda, M. A., Balsamo, G., Bauer, P., Bechtold, P., Beljaars, A. C. M., van de Berg, L., Bidlot, J.,
606 Bormann, N., Delsol, C., Dragani, R., Fuentes, M., Geer, A. J., Haimberger, L., Healy, S. B., Hersbach,
607 H., Holm, E. V., Isaksen, L., Kallberg, P., Kohler, M., Matricardi, M., McNally, A. P., Monge-Sanz, B.
608 M., Morcrette, J. J., Park, B. K., Peubey, C., de Rosnay, P., Tavolato, C., Thepaut, J. N. and Vitart, F.:
609 The ERA-Interim reanalysis: Configuration and performance of the data assimilation system, *Q.*
610 *J. R. Meteorol. Soc.*, 137(656), 553–597, doi:10.1002/qj.828, 2011.

611 Ding, Q., Steig, E. J., Battisti, D. S. and Küttel, M.: Winter warming in West Antarctica caused by
612 central tropical Pacific warming, *Nat. Geosci.*, 4(6), 398–403, doi:10.1038/ngeo1129, 2011.

613 Dixon, D. A., Mayewski, P. A., Goodwin, I. D., Marshall, G. J., Freeman, R., Maasch, A. and Sneed, S.
614 B.: An ice-core proxy for northerly air mass incursions into West Antarctica, *Int. J. Climatol.*, 32,

615 1455–1465, doi:10.1002/joc.2371, 2012.

616 Faegri, K. and Iverson, J.: Textbook of pollen analysis, Blackwell, Oxford., 1975.

617 Fletcher, M.-S. and Moreno, P. I.: Have the Southern Westerlies changed in a zonally symmetric
618 manner over the last 14,000 years? A hemisphere-wide take on a controversial problem, *Quat.*
619 *Int.*, 253, 32–46, doi:10.1016/j.quaint.2011.04.042, 2012.

620 Fogt, R. L., Wovrosh, A. J., Langen, R. A. and Simmonds, I.: The characteristic variability and
621 connection to the underlying synoptic activity of the Amundsen-Bellingshausen Seas Low, *J.*
622 *Geophys. Res. Atmos.*, 117(7), 1–22, doi:10.1029/2011JD017337, 2012.

623 Grimm, E. C.: CONISS: A Fortran 77 Program for stratigraphically constrained cluster analysis by
624 the method of incremental sum of squares, *Comput. Geosci.*, 13(1), 13–35, 1987.

625 Hafsten, U.: The Quaternary history of vegetation in the South Atlantic Islands, *Philos. Trans. R.*
626 *Soc. B*, 152(949), 516–529, doi:10.1098/rspb.1960.0059, 1960.

627 Hancock, G. J., Leslie, C., Everett, S. E., Tims, S. G., Brunskill, G. J. and Haese, R.: Plutonium as a
628 chronomarker in Australian and New Zealand sediments: A comparison with ¹³⁷Cs, *J. Environ.*
629 *Radioact.*, 102(10), 919–929, doi:10.1016/j.jenvrad.2009.09.008, 2011.

630 Hogg, A. G., Hua, Q., Blackwell, P. G., Niu, M., Buck, C. E., Guilderson, T. P., Heaton, T. J., Palmer, J.
631 G., Reimer, P. J., Reimer, R. W., Turney, C. S. M. and Zimmerman, S. R. H.: SHCAL13 Southern
632 Hemisphere calibration, 0–50,000 years cal BP, *Radiocarbon*, 55(4), 1889–1903, 2013.

633 Hosking, J. S., Orr, A., Marshall, G. J., Turner, J. and Phillips, T.: The influence of the amundsen-
634 bellingshausen seas low on the climate of West Antarctica and its representation in coupled
635 climate model simulations, *J. Clim.*, 26(17), 6633–6648, doi:10.1175/JCLI-D-12-00813.1, 2013.

636 Hua, Q. and Barbetti, M.: Review of tropospheric bomb ¹⁴C data for carbon cycle modeling and
637 age calibration purposes, *Radiocarbon*, 46(4), 1273–1298, 2004.

638 IPCC AR5: Climate Change 2013: The Physical Science Basis. Contribution of Working Group I to
639 the Fifth Assessment Report of the Intergovernmental Panel on Climate Change [], edited by T. F.
640 Stocker, D. Qin, G.-K. Plattner, M. Tignor, S. K. Allen, J. Boschung, A. Nauels, Y. Xia, V. Bex, and P.
641 M. Midgley, Cambridge University Press, Cambridge, United Kingdom and New York NY, USA.,

642 2013.

643 Jones, J. M., Gille, S. T., Goosse, H., Abram, N. J., Canziani, P. O., Charman, D. J., Clem, K. R., Crosta,
644 X., Lavergne, C. de, Eisenman, I., England, M. H., Fogt, R. L., Frankcombe, L. M., Marshall, G. J.,
645 Masson-Delmotte, V., Morrison, A. K., Orsi, A. J., Raphael, M. N., Renwick, J. A., Schneider, D. P.,
646 Simpkins, G. R., Steig, E. J., Stenni, B., Swingedouw, D. and Vance, T. R.: Assessing recent trends in
647 high-latitude Southern Hemisphere surface climate, *Nat. Clim. Chang.*, 6(10), 917–926,
648 doi:10.1038/nclimate3103, 2016a.

649 Jones, P. D., Harpham, C. and Lister, D.: Long-term trends in gale days and storminess for the
650 Falkland Islands, *Int. J. Climatol.*, 36(3), 1413–1427, doi:10.1002/joc.4434, 2016b.

651 Juggins, S.: rioja: Analysis of Quaternary Science Data, R package, 2017.

652 Kreutz, K. J., Mayewski, P. A., Pittalwala, I. ., Meeker, L. D., Twickler, M. S. and Whitlow, S. I.: Sea
653 level pressure variability in the Amundsen Sea region inferred from a West Antarctic
654 glaciochemical record, *J. Geophys. Res.*, 105(D3), 4047–4059, 2000.

655 Lachlan-Cope, T. and Connolley, W.: Teleconnections between the tropical Pacific and the
656 Amundsen- Bellinghausens Sea: Role of the El Nino / Southern Oscillation, *J. Geophys. Res.*, 111,
657 D23101, doi:10.1029/2005JD006386, 2006.

658 Lamy, F., Kilian, R., Arz, H. W., Francois, J., Kaiser, J. and Prange, M.: Holocene changes in the
659 position and intensity of the southern westerly wind belt, *Nat. Geosci.*, 3(10), 695–699,
660 doi:10.1038/ngeo959, 2010.

661 Landschützer, P., Gruber, N., Haumann, F. A., Rödenbeck, C., Bakker, D. C. E., Heuven, S. Van,
662 Hoppema, M., Metzl, N., Sweeney, C. and Takahashi, T.: The reinvigoration of the Southern Ocean
663 carbon sink, *Science*, 349(6253), 1221–1224, 2015.

664 Laskar, J., Robutel, P., Joutel, F., Gastineau, M., Correia, a. C. M. and Levrard, B.: A long-term
665 numerical solution for the insolation quantities of the Earth, *Astron. Astrophys.*, 428(1), 261–
666 285, doi:10.1051/0004-6361:20041335, 2004.

667 Lister, D. and Jones, P.: Long-term temperature and precipitation records from the Falkland
668 Islands, *Int. J. Climatol.*, 35(7), 1224–1231, doi:10.1002/joc.4049, 2014.

669 Makou, M. C., Eglinton, T. I., Oppo, D. W. and Hughen, K. A.: Postglacial changes in El Niño and La
670 Niña behavior, *Geology*, 38(1), 43–46, doi:10.1130/G30366.1, 2010.

671 Marshall, G. J.: Trends in the Southern Annular Mode from observations and reanalyses, *J. Clim.*,
672 16(24), 4134–4143, doi:10.1175/1520-0442(2003)016<4134:TITSAM>2.0.CO;2, 2003.

673 Mayewski, P. A., Carleton, A. M., Birkel, S. D., Dixon, D., Kurbatov, A. V., Korotkikh, E., McConnell, J.,
674 Curran, M., Cole-dai, J., Jiang, S. and Plummer, C.: Ice core and climate reanalysis analogs to
675 predict Antarctic and Southern Hemisphere climate changes, *Quat. Sci. Rev.*, 155, 50–66,
676 doi:10.1016/j.quascirev.2016.11.017, 2017.

677 Mayewski, P. A., Maasch, K. A., Dixon, D., Sneed, S. B., Oglesby, R., Korotkikh, E., Potocki, M.,
678 Grigholm, B., Kreutz, K., Kurbatov, A. V., Spaulding, N., Stager, J. C., Taylor, K. C., Steig, E. J., White,
679 J., Bertler, N. A. N. and Jan, R.: West Antarctica’s Sensitivity to Natural and Human-forced Climate
680 Change Over the Holocene, *J. Quat. Sci.*, 28(1), 40–48, doi:10.1002/jqs.2593, 2013.

681 Meehl, G. A., Arblaster, J. M., Bitz, C. M., Chung, C. T. Y. and Teng, H.: Antarctic sea-ice expansion
682 between 2000 and 2014 driven by tropical Pacific decadal climate variability, *Nat. Geosci.*, 9(8),
683 590–595, doi:10.1038/ngeo2751, 2016.

684 Mildenhall, D. C.: Exotic pollen rain on the Chatham Islands during the late pleistocene, *New
685 Zeal. J. Geol. Geophys.*, 19(3), 327–333, doi:10.1080/00288306.1976.10423562, 1976.

686 Moreno, P. I., François, J. P., Villa-Martinez, R. P. and Moy, C. M.: Millennial-scale variability in
687 Southern Hemisphere westerly wind activity over the last 5000 years in SW Patagonia, *Quat. Sci.
688 Rev.*, 28, 25–38, doi:10.1016/j.quascirev.2008.10.009, 2009.

689 Moreno, P. I., Villa-martínez, R., Cárdenas, M. L. and Sagredo, E. A.: Deglacial changes of the
690 southern margin of the southern westerly winds revealed by terrestrial records from SW
691 Patagonia (52 S), *Quat. Sci. Rev.*, 41, 1–21, doi:10.1016/j.quascirev.2012.02.002, 2012.

692 van Oldenborgh, G. J. and Burgers, G.: Searching for decadal variations in ENSO precipitation
693 teleconnections, *Geophys. Res. Lett.*, 32(15), 1–5, doi:10.1029/2005GL023110, 2005.

694 Pike, J., Swann, G. E. A., Leng, M. J. and Snelling, A. M.: Glacial discharge along the west Antarctic
695 Peninsula during the Holocene, *Nat. Geosci.*, 6(3), 199–202, doi:10.1038/ngeo1703, 2013.

696 Pritchard, H. D., Ligtenberg, S. R. M., Fricker, H. A., Vaughan, D. G., Broeke, M. R. Van Den and
697 Padman, L.: Antarctic ice-sheet loss driven by basal melting of ice shelves, *Nature*, 484(7395),
698 502–505, doi:10.1038/nature10968, 2012.

699 Le Quéré, C., Rödenbeck, C., Buitenhuis, E. T., Conway, T. J., Langenfelds, R., Gomez, A.,
700 Labuschagne, C., Ramonet, M., Nakazawa, T., Metz, N., Gillett, N. and Heimann, M.: Saturation of
701 the Southern Ocean CO₂ Sink Due to Recent Climate Change, *Science*, 316(1994), 1735–1738,
702 2007.

703 Raphael, M. N., Marshall, G. J., Turner, J., Fogt, R. L., Schneider, D., Dixon, D. A., Hosking, J. S.,
704 Jones, J. M. and Hobbs, W. R.: THE AMUNDSEN SEA LOW: Variability, Change, and Impact on
705 Antarctic Climate, *Bull. Am. Meteorol. Soc.*, January, 111–122, doi:10.1175/BAMS-D-14-00018.1,
706 2016.

707 Rein, B., Lu, A., Reinhardt, L., Sirocko, F., Wolf, A., Dullo, W. C., Nin, E., Lückge, A., Reinhardt, L.,
708 Sirocko, F., Wolf, A. and Dullo, W. C.: El Niño variability off Peru during the last 20,000 years,
709 *Paleoceanography*, 20, 1–18, doi:10.1029/2004PA001099, 2005.

710 Russell, A. and McGregor, G. R.: Southern hemisphere atmospheric circulation: Impacts on
711 Antarctic climate and reconstructions from Antarctic ice core data, *Clim. Change*, 99(1), 155–
712 192, doi:10.1007/s10584-009-9673-4, 2010.

713 Schneider, D. P., Deser, C. and Okumura, Y.: An assessment and interpretation of the observed
714 warming of West Antarctica in the austral spring, *Clim. Dyn.*, 38, 323–347, doi:10.1007/s00382-
715 010-0985-x, 2012.

716 Sime, L. C., Kohfeld, K. E., Le, C., Wolff, E. W., Boer, A. M. De, Graham, R. M. and Bopp, L.: Southern
717 Hemisphere westerly wind changes during the Last Glacial Maximum: model-data comparison,
718 *Quat. Sci. Rev.*, 64(2013), 104–120, doi:10.1016/j.quascirev.2012.12.008, 2010.

719 Thomas, Z. A.: Using natural archives to detect climate and environmental tipping points in the
720 Earth System, *Quat. Sci. Rev.*, 152, 60–71, doi:10.1016/j.quascirev.2016.09.026, 2016.

721 Thomas, Z., Turney, C., Allan, R., Colwell, S., Kelly, G., Lister, D., Jones, P., Beswick, M., Alexander,
722 L., Lippmann, T., Herold, N. and Jones, R.: A new daily observational record from Grytviken,

723 South Georgia: exploring 20th century extremes in the South Atlantic, *J. Clim.*, 31, 1743–1755,
724 doi:10.1175/JCLI-D-17-0353.1, 2018.

725 Thompson, D. W. J., Solomon, S., Kushner, P. J., England, M. H., Grise, K. M. and Karoly, D. J.:
726 Signatures of the Antarctic ozone hole in Southern Hemisphere surface climate change, *Nat.*
727 *Geosci.*, 4(11), 741–749, doi:10.1038/ngeo1296, 2011.

728 Turner, J., Lu, H., White, I., King, J. C., Phillips, T., Hosking, J. S., Bracegirdle, T. J., Marshall, G. J.,
729 Mulvaney, R. and Deb, P.: Absence of 21st century warming on Antarctic Peninsula consistent
730 with natural variability, *Nature*, 535(7612), 411–415, doi:10.1038/nature18645, 2016.

731 Turner, J., Phillips, T., Hosking, J. S., Marshall, G. J. and Orr, A.: The Amundsen Sea low, *Int. J.*
732 *Bifurc. Chaos*, 1829, 1818–1829, doi:10.1002/joc.3558, 2013.

733 Turney, C. S. M., Fogwill, C. J., Palmer, J. G., Sebille, E. Van, Thomas, Z., Mcglone, M., Richardson, S.,
734 Wilmshurst, J. M., Fenwick, P., Zunz, V., Goosse, H., Wilson, K., Carter, L., Lipson, M., Jones, R. T.,
735 Harsch, M. and Clark, G.: Tropical forcing of increased Southern Ocean climate variability
736 revealed by a 140-year subantarctic temperature reconstruction, *Clim. Past*, 13, 231–248,
737 doi:10.5194/cp-13-231-2017, 2017a.

738 Turney, C. S. M., Jones, R., Fogwill, C., Hatton, J., Williams, a. N., Hogg, A., Thomas, Z., Palmer, J.
739 and Mooney, S.: A 250 year periodicity in Southern Hemisphere westerly winds over the last
740 2600 years, *Clim. Past*, 12, 189–200, doi:10.5194/cpd-11-2159-2015, 2016a.

741 Turney, C. S. M., Jones, R. T., Lister, D., Jones, P., Williams, A. N., Hogg, A., Thomas, Z. A., Compo, G.
742 P., Yin, X., Fogwill, C. J., Palmer, J., Colwell, S., Allan, R. and Visbeck, M.: Anomalous mid-twentieth
743 century atmospheric circulation change over the South Atlantic compared to the last 6000
744 years, *Environ. Res. Lett.*, 11(6), 064009, doi:10.1088/1748-9326/11/6/064009, 2016b.

745 Turney, C. S. M., Wilmshurst, J. M., Jones, R. T., Wood, J. R., Palmer, J. G., Hogg, A. G., Fenwick, P.,
746 Crowley, S. F., Privat, K. and Thomas, Z.: Reconstructing atmospheric circulation over southern
747 New Zealand: Establishment of modern westerly air flow 5500 years ago and implications for
748 Southern Hemisphere Holocene climate change, *Quat. Sci. Rev.*, 159, 77–87,
749 doi:10.1016/j.quascirev.2016.12.017, 2017b.

750 Upson, R., Williams, J. J., Wilkinson, T. P., Clubbe, C. P., Ilya, M., Maclean, D., Mcadam, J. H. and
751 Moat, J. F.: Potential Impacts of Climate Change on Native Plant Distributions in the Falkland
752 Islands, PLoS One, 11, e0167026., doi:10.1371/journal.pone.0167026, 2016.

753 Villa-martínez, R., Moreno, P. I. and Valenzuela, M. A.: Deglacial and postglacial vegetation
754 changes on the eastern slopes of the central Patagonian Andes (47 S), Quat. Sci. Rev., 32(2012),
755 86–99, doi:10.1016/j.quascirev.2011.11.008, 2012.

756 Visbeck, M.: A station-based southern annular mode index from 1884 to 2005, J. Clim., 22(4),
757 940–950, doi:10.1175/2008JCLI2260.1, 2009.

758 Wace, N. . and Dickson, J. .: Part II. The terrestrial botany of the Tristan da Cunha Islands, Philos.
759 Trans. R. Soc. B, 249, 273–360, doi:10.1098/rstb.1965.0014, 1965.

760 Wessel, P., Smith, W. H. F., Scharroo, R., Luis, J. and Wobbe, F.: Generic Mapping Tools: Improved
761 Version Released, Eos, Trans. Am. Geophys. Union, 94(45), 409–410,
762 doi:10.1002/2013EO450001, 2013.

763 Wilson, P., Clark, R., Birnie, J. and Moore, D. M.: Late Pleistocene and Holocene landscape
764 evolution and environmental change in the Lake Sullivan area, Falkland Islands, South Atlantic,
765 Quat. Sci. Rev., 21(16–17), 1821–1840, doi:10.1016/S0277-3791(02)00008-2, 2002.

766

Anonymous Referee #1 Received and published: 20 April 2018

Thomas et al. present new high-resolution pollen data on a radiocarbon dated peat record from the Falkland Islands for the last about 5000 years. They relate major changes in the vegetation dynamics on the island and in the far-distant Patagonia pollen transport to major reorganizations of the high latitude Antarctic atmospheric circulation pattern in the Southeastern Pacific sector, namely the intensity and position of the Amundsen Sea Low (ASL).

Main observation of this study is a significant change in the vegetation and enhanced charcoal input around 2.5 kyrs indicating a shift to warmer/drier conditions over the island likely associated with a strengthening and northward expansion of the ASL. Simple Dome ice core data and a marine carbonate record from the Chilean fjord region are used for comparison and in support of their interpretation. This peat record is one of the few very valuable paleoenvironmental data available from this part of the world. However, this cannot be the only reason to assume, that it is representative for the whole South Atlantic (“across the South Atlantic”), as it is stated several time in the manuscript. Rather it responds to SE Pacific/Southern Ocean climate variability, which is restricted more or less to the southeastern South Atlantic (as it is shown also in the correlation maps, Fig. 2). Altogether, the manuscript is well organized and concise, referencing is adequate, and the layout and total number of figures are very reasonable.

We thank the reviewer for their kind remarks and constructive suggestions, which have been extremely helpful for improving our manuscript. We have addressed all the comments in the revised manuscript and detail these below. (Our responses in blue, reviewer comments in black).

General remarks:

1. Please provide evidence for the representativeness of this location for the South Atlantic, if not please correct the respective statements in the whole manuscript

We understand the reviewers concern here and stated more explicitly the importance of the location and our interpretation of the results. Crucially, the Falkland Islands lie at a strategic location sensitive to changes in the Amundsen Sea Low, through the influence of the latter on atmospheric circulation over the southeastern South Atlantic region (e.g. Fogt et al. 2012, Russell and McGregor 2010, Hosking et al. 2013 and Turner et al. 2013).

2. The indicated wind pattern in figure 1 is too simplistic and this map would benefit from adding major surface current patterns and the frontal zones in this region.

This is a good suggestion. We have added the 925 hPa winds (vectors) trends since 1979 from ERA-Interim (Dee et al., 2011). This shows both the location and increase in westerly winds over the satellite era. We have also added the mean locations of the southern limb of the Antarctic Circumpolar Current (purple), the polar front (red) and the subantarctic front (green), following Orsi et al. (1995). (See the revised Figure 1 below).

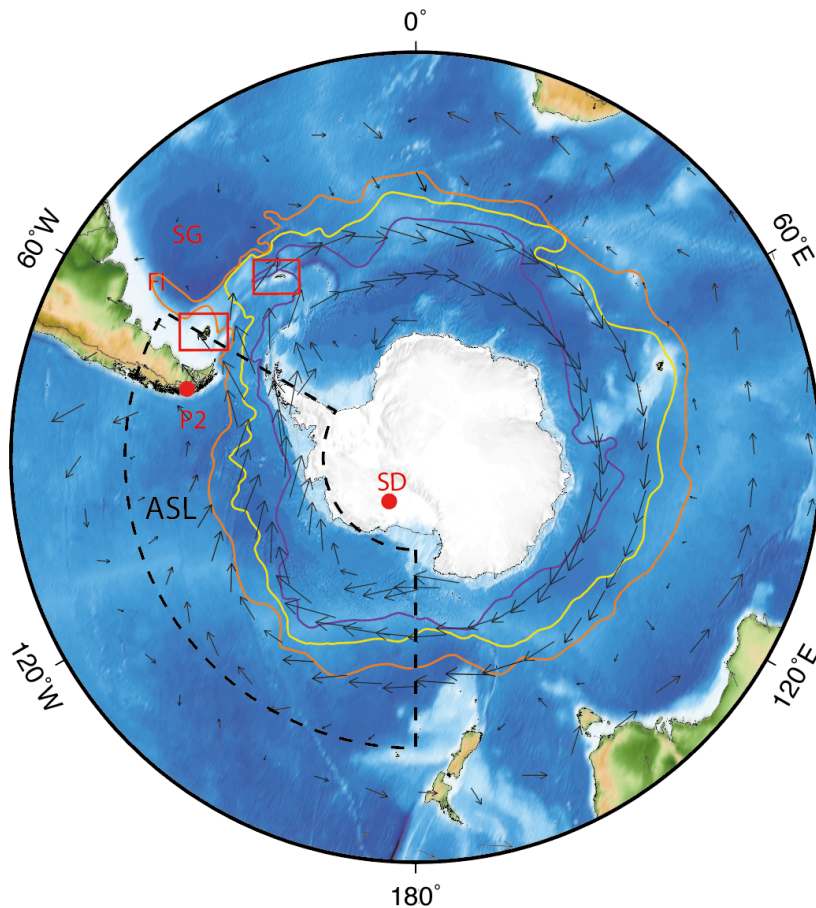


Figure 1. Location of the Falkland Islands (FI), South Georgia [SG], Siple Dome [SD] and Palm 2 [P2]. Dashed line denotes contemporary defined limits of the ASL domain (Fogt et al., 2012). Mean locations of the southern limb of the Antarctic Circumpolar Current (purple), the polar front (red) and the subantarctic front (green) are shown, following Orsi et al. (1995). The grey arrows denote the 925 hPa winds (vectors) trends since 1979 from ERA-Interim (Dee et al., 2011), depicting the location and increase in westerly winds over the satellite era. Map made using Generic Mapping Tools (GMT) (Wessel et al., 2013).

3. The interpretation of the own data is very much restricted to the atmospheric part. Changes in ACC strength, Drake Passage through flow, and the surface current dynamics in the southwestern South Atlantic (Malvinas confluence dynamics e.g. Voigt et al. 2015) are important as well and not discussed.

We appreciate the reviewers concern. Our analysis demonstrates the dominant control on temperature and precipitation at Canopus Hill is via atmospheric processes. Spatial correlation maps suggest limited ocean influence on these climate variables on the Falkland Islands; something we have now stated explicitly. As part of this we have added a discussion of ocean currents, and have also added the mean locations of the southern limb of the Antarctic Circumpolar Current (purple), the polar front (red) and the subantarctic front (green), following Orsi et al. (1995), to Figure 1. We feel a figure showing this does not add to the narrative but if the editor would like us to include we are happy to do so.

4. Regarding the age model I have two comments/remarks. One is regarding the ^{137}Cs record. It is mentioned in the text as age marker for the early sixties nuclear weapon testing fallout. Normally, the manuscript should contain the graphic display of the whole measured activity profile, just the mentioning in the text is not enough. Second, if fruits and leaves were ^{14}C dated (as indicated in the table), there is not much reason to exclude two dated at the base but include only the one date above (this could have been an outlier as well). Sedimentation rates would make sense with the two basal xsages as well. So I suggest to include them into the Bayesian age modelling.

We thank the reviewer for their suggestions to improve the description of the age modelling. As commented in Hancock et al. (2011), the anthropogenic radionuclide, ^{137}Cs (with a half time of 30 years) is derived from atmospheric nuclear weapons testing and can provide an important “first appearance” horizon of known age (1954–1955) i.e. an independent marker horizon to assist with age model validation. Specifically, we analysed contiguous peat samples for the first presence of ^{137}Cs and in the age model used the prior U(1952, 2011) to capture the possible range of calendar years (CE) for the onset of ^{137}Cs deposition in the sequence (Hancock et al 2011). We have however, included more detail on the measurement and application of ^{137}Cs for constructing our age model.

We agree that we should have explained in more details why the two basal ages were removed. The sedimentation rate is internally more consistent when excluding these two basal ages; without them the sedimentation rate from the entire metre of sediment above does not change significantly (with a sedimentation rate for 141.5-156 cm of 38 yrs/cm compared to an average of 27 yrs/cm for the preceding metre of sediment), whereas including them increases the sedimentation rate over this depth range abruptly to 11.6 yrs/cm. We suspect these basal ages may comprise some intruded younger root material; a scenario not unusual in relatively slowly accumulating sedimentary sequences e.g. Brock et al. (2011, *Quaternary Geochronology*). However, we have run the age model again to include these basal ages, and have added a column in Table 1 include the mean calibrated 2 sigma age range. The calibrated age ranges are almost identical for both age models until 142 cm, from where it diverges. Importantly, our conclusions based on the changes observed in the Canopus Hill Record at ~2.5 ka BP are not at all affected by the choice of age model. The modified Table 1 is pasted below:

Depth, cm	Wk lab number	Material	% Modern ^{14}C BP $\pm 1 \sigma$	2 σ cal. age range (years BP)	2 σ cal. age range (years BP)	Mean cal. age (years BP)
				With 2 basal ages	Excluding 2 basal ages	
8-9	34598	Fruits and leaves	117.0 \pm 0.4%M	-4 to -43	-4 to -44	-21
9		^{137}Cs		-6 to -42	-6 to -42	-19
11-12	32994	Fruits and leaves	107.8 \pm 0.4%M	-2 to -14	-1 to -14	-8
18-19	37007	Fruits and leaves	107.3 \pm 0.3%M	0 to -13	26 to -15	-3
25-26	35146	Fruits and leaves	95 \pm 25	250 to -1	249 to -1	86
35-36	37008	Fruits and leaves	647 \pm 25	652 to 547	652 to 547	603
39-40	33445	Fruits and leaves	761 \pm 25	719 to 570	719-570	661
57-58	32996	Fruits and leaves	1818 \pm 25	1804 to 1595	1801 to 1597	1682
70-71	32350	Fruits and leaves	2235 \pm 25	2315 to 2102	2314 to 2104	2215
97-98	32997	Fruits and leaves	2749 \pm 25	2866 to 2755	2865 to 2755	2810
107-108	32998	Fruits and leaves	2914 \pm 26	3140 to 2877	3139 to 2878	2997
120-121	41767	Fruits and leaves	3238 \pm 20	3476 to 3361	3471 to 3362	3416
141-142	32351	Fruits and leaves	3955 \pm 32	4430 to 4184	4511 to 4236	4352
148-149	41768	Fruits and leaves	4390 \pm 20	4515 to 4300	5027 to 4845	4908
153.5-154.5	42144	Fruits and leaves	4039 \pm 21	4521 to 4421		
156.5-157.5	42145	Fruits and leaves	4075 \pm 22	4567 to 4429		

Table 1. Radiocarbon and modelled calibrated age ranges for the Canopus Hill peat sequences using the *P*-sequence and Outlier analysis option in OxCal 4.2 (Bronk Ramsey, 2008; Bronk Ramsey and Lee, 2013). The SHCal13 (Hogg et al., 2013) and Bomb04SH (Hua and Barbetti, 2004) calibration curves were used. Note: calibrated ages are relative to Before Present (BP) i.e. CE 1950.

5. In the “contemporary climate” chapter the author use deseasonalised/detrended seasonal data? As a paleoclimatologist, I’s difficult for me to understand this preprocessing step and perhaps some additional explanation could make things clearer here.

This is a fair point. Using deseasonalised and detrended data means that the correlations between two records are not based on them having similar seasonal differences, or similar trends, which would bias the correlation. We have included a more detailed explanation in the main manuscript to explain this. Thank you for the suggestion to make this clearer.

6. In the data comparison chapter the Siple Dome and PALM2 data are assumed to be consistent with the Falkland data. There are, however, rather large offsets in the timing of the proposed “regime shift”. Majewski et al. e.g. suggest the Siple Dome ssNa⁺ shift to start around 1000-1500 years BP - that is more than 1000 years later than the quite abrupt shift described in the Canopus Hill record. There is also a 500 year offset to the carbonate accumulation record from the Chilean Fjords, which, by the way, is not an accumulation of carbonate in the surficial fjord waters, neither a carbonate preservation issue. If I understood these authors well, it represents marine carbonate production in the surficial fjord waters and its subsequent accumulation on the sea bed in response to salinity changes in the upper water column of the fjord. Of course all these records have their own stratigraphic issues, but one perhaps should discuss the potential meaning of these offsets more thoroughly.

We acknowledge there are differences in the timing within the records that we compare. These may be an artefact of the uncertainties in the individual age models, or represent real dynamic changes operating on multi-decadal to centennial timescales. Importantly, we now make clear we are not specifically suggesting that there is a ‘regime shift’ that affects the entire region concurrently. Indeed, the Siple Dome ssNa⁺ record shows a more long-term trend to a deepening of the ASL that may suggest an early expression in this part of the Antarctic (as shown in Figure 4). Identifying a particularly time for a shift may be misleading, and we have removed any reference to a specific age.

In terms of the PALM2 record (and other records that we have since added from the Peruvian margin), there changes do appear to be more abrupt, and several centuries after the observed shift in the Canopus Hill record. We have included a significantly more detailed discussion on the timing of these changes. We have also reworded the description of the PALM2 record to be clearer, thank you.

7. The Late Holocene changes described in Lamy et al. address the latitudinal northward displacement of the westerly wind strength from its southern core (Early Holocene) towards its northern margin (Late Holocene). Conceptually, they suggest a weakening of the core westerlies in the Magellan Strait region, which is somehow in contradiction to what the authors assume in this manuscript.

In terms of comparisons to other reconstructions of westerly airflow, there is a substantial incongruity between different proxy records over the Holocene. It must also be pointed out that while the Lamy et al. reconstruction covers the full Holocene, the new extended record from Canopus Hill only covers the last 5000 years; thus comparisons between the early and late Holocene are not possible. The Lamy et al. (2010) paper does seem to indicate stronger westerly airflow from ~2 ka BP, which may have been influenced by the ASL, however, the last age control point for this record is the start of the inflection, which is dated to 2570 ¹⁴C BP, calibrated to 2410 cal yr BP (note however that no uncertainty or calibrated age range is given, nor is there a reported uncertainty for the marine reservoir correction of 200 years). This indicates that the age uncertainties between the changes observed in the Canopus Hill record and the PALM2 record may possibly overlap.

8. Beside the millennial-scale trend there is much more centennial-scale fluctuation in the pollen/charcoal data from Falkland Island that unfortunately are not discussed.

While there is discussion in Turney et al. (2016) with regards to the centennial-scale variability identified in Canopus Hill, we agree that this should be briefly discussed. In addition, similar cyclical variations in West Antarctic Peninsula glacier discharge in Pike et al. (2013, *Nature Geoscience*) have also been reported; something not discussed in the previous draft of the manuscript but is now included.

Minor comments:

Line 30: please explain why ASL is of global significance.

A fair point, we did not explain this well. We have reworded the beginning of the abstract to introduce the ASL better.

Line 98: More precisely it is a vegetation record. “record of airflow” is for my feeling to imprecise here

We do understand the reviewers point here, however, we strongly believe it is more appropriate to call it a record of airflow. In particular, the *Nothofagus* and charcoal is emphatically not a record of vegetation change on the Falkland Islands (being wind-blown from South America), and it would be incorrect to discuss it in this way. It is true however that the local pollen does represent vegetation on the Falkland Islands. We will be more explicit about the interpretation of the proxies depending on whether they represent local or ‘exotic’ sources.

Line 133: If mentioned, please provide the exact information for the two periods

We are unsure what the reviewer means here, though we infer that it is the period defining the contemporary limits of the ASL and oceanic fronts. Assuming this is correct, we have added this information: The contemporary limits of the ASL (45-75°S, 180-60°W) are defined across the 1979–2001 average (Fogt et al., 2012), while the Orsi et al. (1995) oceanic front data is based on analyses of hydrographic station data available up to 1990 (see Table 1 of Orsi et al. 1995 for more details). We hope this satisfactory.

Line 125: “contiguously” should be “continuously”

In fact we do mean ‘contiguously’ here (differing from ‘continuously’ to mean having discrete boundaries between each sample, i.e. every cm).

Line 283-283: This cannot be, except the authors assume an full inversion of the westerly winds? Across the South Atlantic would mean easterly winds?

We think there may be some confusion here. From a climate/meteorological context, west to east airflow is described as ‘westerly winds’, i.e. from the west.

Line 291: “compliment” should be “complement”

We have changed this, thank you.

Anonymous Referee #2 Received and published: 26 September 2018

The authors present a new blanket peat record from Canopus Hill, Falkland Islands, to reconstruct changes in the in the Amundson Sea Low (ASL) and the Southern Annual Mode. The new record from Canopus Hill extend previously published results (Turney et al., 2016) to the mid-Holocene. The new record suggests a major shift of the ASL at around 2.5 kyr BP, as previously stated by Turney et al (2016). The main results presented in this study are therefore not really original and are therefore not a major advancement. The comparison of the Canopus Hill record with other records show some differences in the timing of this major change, which however are not really discussed in the manuscript. Overall, the manuscript require major revisions (see detailed comments below).

We thank the reviewer for their comments, which have helped clarify our manuscript. (Our responses in blue, reviewer comments in black). We suspect there may be some confusion regarding the Turney et al. (2016) paper, which presents a record only 2.5 kyr long, and therefore does not (and could not!) report a shift at 2.5 ka BP. We think this confusion may be a result of the sentence at line 125-127: “*Work at this site has previously recognised the input of exotic pollen and charcoal derived from South America (Turney et al., 2016a), with changes to westerly airflow over the past ~2.5 ka.*” We appreciate that this sentence is confusing, and we sincerely apologise for this oversight. The sentence was only intended to convey the fact that exotic pollen has been previously identified at this site over the length of the Turney et al. (2016) record, which had only been analysed back to 2.5 kyr ago. It is an unfortunate and confusing coincidence that the changes we see in this manuscript occur at the limit of the Turney et al. (2016) study. We have changed this sentence to ensure that it does not promote confusion to “*Work at this site has previously recognised the input of exotic pollen and charcoal derived from South America but was limited to the last 2.5 kyr (Turney et al., 2016a).*”

Importantly, in terms of the originality of the manuscript, the South Atlantic is traditionally interpreted in terms of westerly wind strength changes. Here we report the first Atlantic record that recognises changes in the Amundsen Sea Low through the mid to late Holocene. We have ensured this finding is highlighted more clearly. Viewing the CPD metrics, the discussion paper has been viewed more than 377 times, demonstrating the interest in this topic. Both reviews have made excellent suggestions to improve the clarity and we believe the manuscript has been significantly improved.

1) The current age model and its uncertainties are not very well presented and it remains unclear why two radiocarbon ages at the base of the sequence were omitted. These ages are clearly not in stratigraphic order and the authors should provide plausible explanations for this mismatch. The 2-sigma age range should be also given in table 1 to allow readers to evaluate the chronological age uncertainties.

We have added more detail on the construction of the age model, and included the 2-sigma age range. However, the only radiocarbon ages that are not in stratigraphic order are the two basal ages that were excluded, though we agree that we should have explained in more detail why the two basal ages were removed. The sedimentation rate is internally more consistent when excluding these two basal ages; without them the sedimentation rate from the entire metre of sediment above does not change significantly (with a sedimentation rate for 141.5-156 cm of 38 yrs/cm compared to an average of 27 yrs/cm for the preceding metre of sediment), whereas including them increases the sedimentation rate over this depth range abruptly to 11.6 yrs/cm. We suspect these basal ages may comprise some intruded younger root material; a scenario not unusual in relatively slowly accumulating sedimentary sequences e.g. Brock et al. (2011, *Quaternary Geochronology*). However, we have run the age model again to include these basal ages, and have added a column in Table 1 include the mean calibrated 2 sigma age range. The calibrated age ranges are almost identical for both age models until 142 cm, from where it diverges. Importantly, our conclusions based on the changes observed in the Canopus Hill Record at ~2.5 ka BP are not at all affected by the choice of age model. The modified Table 1 is pasted below:

Depth, cm	Wk lab number	Material	% Modern ^{14}C BP $\pm 1 \sigma$	2 σ cal. age range	2 σ cal. age range	Mean cal. age (years BP)	
				(years BP)	(years BP)		
				With 2 basal ages	Excluding 2 basal ages		
8-9	34598	Fruits and leaves	117.0 \pm 0.4%M	-4 to -43	-4 to -44	-21	
9		^{137}Cs		-6 to -42	-6 to -42	-19	
11-12	32994	Fruits and leaves	107.8 \pm 0.4%M	-2 to -14	-1 to -14	-8	
18-19	37007	Fruits and leaves	107.3 \pm 0.3%M	0 to -13	26 to -15	-3	
25-26	35146	Fruits and leaves	95 \pm 25	250 to -1	249 to -1	86	
35-36	37008	Fruits and leaves	647 \pm 25	652 to 547	652 to 547	603	
39-40	33445	Fruits and leaves	761 \pm 25	719 to 570	719-570	661	
57-58	32996	Fruits and leaves	1818 \pm 25	1804 to 1595	1801 to 1597	1682	
70-71	32350	Fruits and leaves	2235 \pm 25	2315 to 2102	2314 to 2104	2215	
97-98	32997	Fruits and leaves	2749 \pm 25	2866 to 2755	2865 to 2755	2810	
107-108	32998	Fruits and leaves	2914 \pm 26	3140 to 2877	3139 to 2878	2997	
120-121	41767	Fruits and leaves	3238 \pm 20	3476 to 3361	3471 to 3362	3416	
141-142	32351	Fruits and leaves	3955 \pm 32	4430 to 4184	4511 to 4236	4352	
148-149	41768	Fruits and leaves	4390 \pm 20	4515 to 4300	5027 to 4845	4908	
153.5-154.5	42144	Fruits and leaves	4039 \pm 21	4521 to 4421			
156.5-157.5	42145	Fruits and leaves	4075 \pm 22	4567 to 4429			

Table 1. Radiocarbon and modelled calibrated age ranges for the Canopus Hill peat sequences using the *P*-sequence and Outlier analysis option in OxCal 4.2 (Bronk Ramsey, 2008; Bronk Ramsey and Lee, 2013). The SHCal13 (Hogg et al., 2013) and Bomb04SH (Hua and Barbetti, 2004) calibration curves were used. Note: calibrated ages are relative to Before Present (BP) i.e. CE 1950.

2) It is not entirely clear how the SAL and the Southern Annual Mode (SAM) are dynamically linked! The authors should discuss this in greater detail in their manuscript.

We apologise that this was not clear in the manuscript. In fact the dynamical links between these two modes of variability are not well understood. While there have been suggested links between strong cyclone events in the Amundsen-Bellinghousen Sea region and the Southern Annular Mode e.g. Fogt et al. (2012), the main modulator is not clear. We have added some more information to the introduction about this, but also go into more detail in the discussion about the links between the SAM, ASL and ENSO (see response to comments 5 and 6).

3) Lines: 230-232: Explain the difference to previous publications (e.g., Turney et al., 2016a), in particular in the representation of Cyperaceae and the total accumulation of pollen centred at 2.5 ka BP. The core presented in Turney et al., 2016 was also collected from Canopus Hill.

We apologise that this was not clear in the manuscript. The data presented in Turney et al. (2016a) was indeed collected from the same site (Canopus Hill). However, this record was only 2.5 kyr long. We have removed the Turney et al. (2016) reference from line 230 as this does add confusion since the sentence does say through the mid- to late-Holocene, which the Turney et al. (2016) record does not infer.

4) Line 267-269: It would be interesting to see a detailed comparison between the charcoal records from Canopus Hill and Patagonia to support the statement that “The aeolian delivery of the charcoal to the Falkland Islands is supported by the close correspondence between the Canopus Hill and Lago Guanaco, Southwest Patagonia (Moreno et al., 2009) charcoal records”. Such a comparison would strengthen the manuscript, and in particular the statement “ Our results support the notion of pervasive westerly winds throughout the mid- to late-Holocene”.

We apologise for the confusion. As intimated in the previous sentence, this observation was intended to convey that Lago Guanaco shows a consistent pattern of pervasive fire in the immediate area in Patagonia over the last 3000 years, with limited expression prior to this time. We have included the Moreno et al. charcoal record in Figure 4 to aid comparison. More importantly the presence of fire in the Patagonian landscape during the late Holocene provides a ready source of exotic material for aerial transport to the Falkland Islands as a result of westerly airflow. We have amended this sentence, and broadened the discussion of *Nothofagus*; the fact that *Nothofagus* is consistently represented throughout the Canopus Hill record indicates pervasive westerly winds throughout the mid to late-Holocene, but does not have sufficiently high concentrations to robustly assess changes.

5) The authors state that “These results compliment other studies from the broader South Atlantic region (Figure 4). “ However, the change in ssNA in Simple Dome are rather smooth, especially when compared to the pollen record. This difference should be explained in more detail, e.g. are the Falkland Islands more sensitive to these changes than Simple Dome. A marked increase in ssNA at around 2.9 ka is hardly visible in the Simple Dome record and pre-dates the vegetation changes at 2.5 ka. What is the reason for the 400 year time lag. Adding the uncertainties of the age estimate of 2.5 kyr in the Canopus Hill record. Furthermore, the increase in the PALM2 record starts even later at around 2kyr BP. The authors should discuss the offsets more carefully and not simply state that a major change in the westerlies occurred at 2.5 kyr as this estimate is not supported by the current evidences. This discrepancy could be either related to dating uncertainties or may hold important information on the spatial-temporal impacts of the ASL/westerlies.

We acknowledge there are differences in the timing within the records that we compare. These may be an artefact of the uncertainties in the individual age models, or represent real dynamic changes operating on multi-decadal to centennial timescales. Importantly, we now make clear we are not specifically suggesting that there is a ‘regime shift’ that affects the entire region concurrently. Indeed, the Simple Dome ssNA+ record shows a more long-term trend to a deepening of the ASL that may suggest an early expression in this part of the Antarctic (as shown in Figure 4). Identifying a particular time for a shift may be misleading, and we have removed any reference to a specific age. The uncertainties of the age estimates for the Canopus Hill record are already plotted in Figure 4, and show that there are relatively large uncertainties of between 100 and 300 years (though the calibrated 2-sigma age range is now clearer to see in Table 1).

However, there does seem to be some confusion regarding the changes at ~2.5 ka BP. We do not state that there is a change in westerlies at 2.5 ka BP, but rather that the changes in vegetation and westerly airflow at Canopus Hill are consistent with the deepening of the ASL. As suggested in point 2, we have added more detail on the dynamical link between the westerlies and the ASL, which provides more context to the discussion. In terms of comparisons to reconstructions of westerly airflow in published literature, there is a substantial incongruity between different proxy records over the Holocene. The Lamy et al. (2010) paper does seem to indicate stronger westerly airflow from ~2 ka BP, which may have been influenced by the ASL, however, the last age control point for this record is the start of the inflection, which is dated to 2570 ¹⁴C BP, calibrated to 2410 cal yr BP (note however that no uncertainty or calibrated age range is given, nor is there a reported uncertainty for the marine reservoir correction of 200 years). This indicates that the age uncertainties between the changes observed in the Canopus Hill record and the PALM2 record may possibly overlap. We will include a significantly more detailed discussion on the timing of these changes.

Interestingly, the $\delta^{18}\text{O}_{\text{diatom}}$ record from Site 1099 in the Palmer Deep representing multi-centennial fluctuations in glacial discharge presented by Pike et al. (2013, *Nature Geoscience*), also shows an underlying decrease towards lower values, “particularly from ~2.5 kyr”. Specifically, this increased glacial ice discharge is thought to have been driven by atmospheric warming (as a result of peak local summer insolation; now added to Figure 4), in addition to the maximum Holocene ENSO frequency from circa 2.2 kyr (suggested by Makou et al. (2010, *Geology*), likely representing increased La Niña intensity (Site 1228 Peru Margin core displays an increase in La Niña events, now plotted in Figure 4). We have added these important details to the discussion.

6) I would also suggest to include ENSO reconstructions (e.g., Moy et al., 2002 or Carre et al., 2014) in a separate figure

This is an excellent idea to include an ENSO reconstruction, although we think it is best to add to Figure 4 to enable better comparisons. Unfortunately, since this paper was submitted, the record of Moy et al. 2002 has been questioned as an El Niño record (Schneider, T., Hampel, H., Mosquera, P. V., Tylmann, W. and Grosjean, M.: Paleo-ENSO revisited: Ecuadorian Lake Pallcacocha does not reveal a conclusive El Niño signal, *Glob. Planet. Change*, 168(June), 54–66, doi:10.1016/j.gloplacha.2018.06.004, 2018.). This study states that ENSO may not be the major driver of precipitation at Lake Pallcacocha, and therefore may not be appropriate to cite in an ENSO context. While Carre et al. (2014) establish that modern ENSO conditions were established between 3 and 4.5 ka BP, this is based on discontinuous records; the record published by Makou et al. (2010 *Geology*) appears to present a more continuous record of ENSO over the time period of interest for this study, and we have included this record in Figure 4. We also significantly broaden our discussion of the potential influence of ENSO on the ASL: The El Niño Southern Oscillation circulation pattern is teleconnected to Southern Ocean and Antarctic climate, in particular the Amundsen Sea low-pressure region, via movements of the South Pacific Convergence Zone (Russel and McGregor et al. 2010, *Climatic Change*). Specifically, La Niña events are accompanied by a northerly shift in the South Pacific Convergence Zone and the production of cyclones in the region of the Amundsen Sea low. This then produces a warm, northerly airflow over Patagonia, the Western Antarctic Peninsula and the Falkland Islands. In addition, Fogt et al. (2011) found that when a La Niña event occurs with the positive phase of the SAM, ASL exhibits deeper pressure anomalies, suggesting that the SAM and the ASL may indeed modulate one another. Please see revised Figure 4 below:

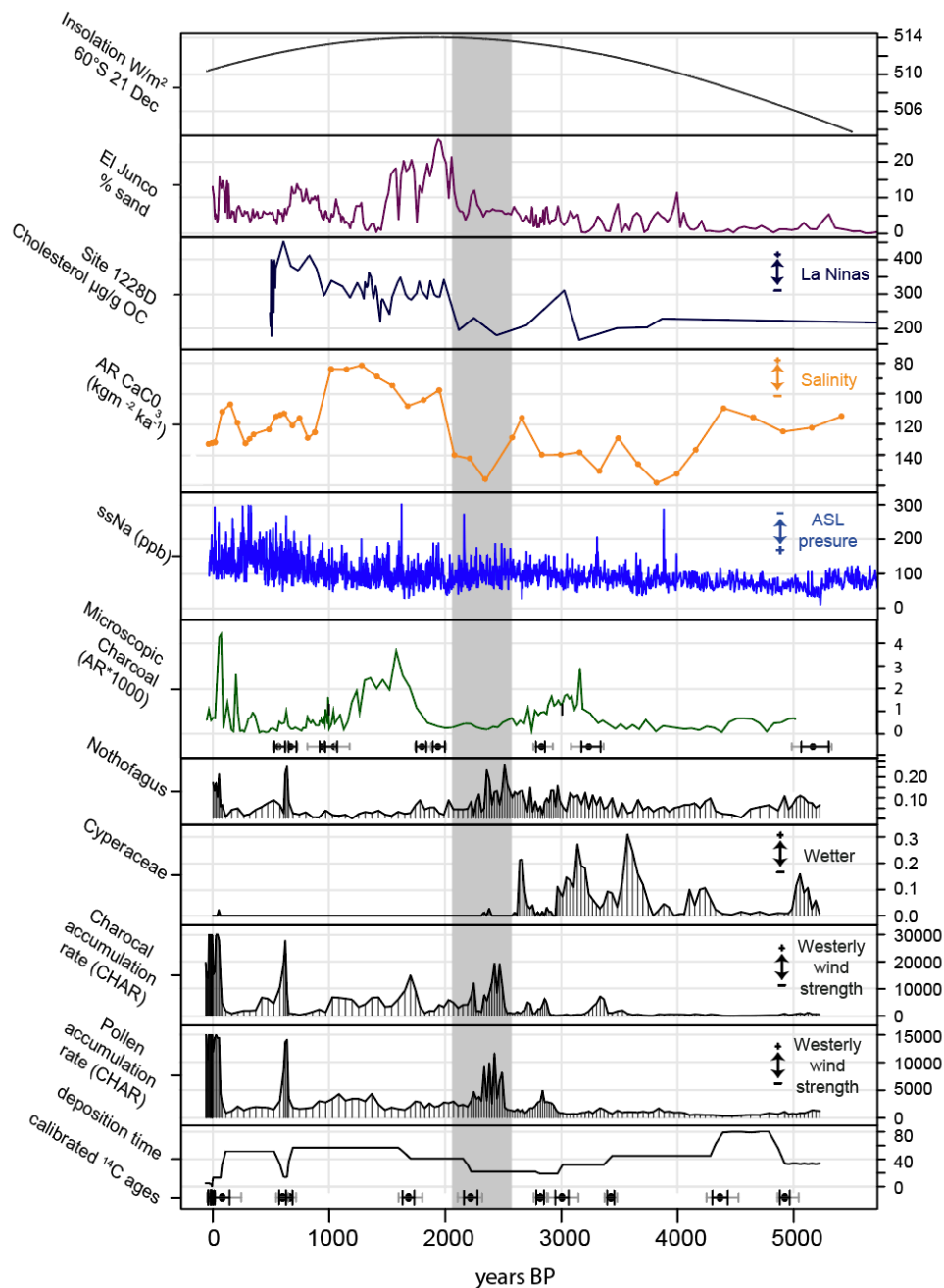


Figure 4: Key data from the Canopus Hill sequence (Falkland Islands) and other South Atlantic records. From bottom to top: deposition time, total pollen accumulation rate (PAR), total charcoal accumulation rate (CHAR), Cyperaceae and Nothofagus re-expressed as accumulation rates, microscopic charcoal from Lago Guanaco (Moreno et al. 2009), ssNa⁺ from Siple Dome (Mayewski et al., 2013), salinity anomalies from PALM2 (Lamy et al., 2010), cholesterol abundance, ODP Site 1228, Peru margin (Makou et al. 2010), percentage of sand, El Junco Crater Lake, Galápagos (Convey et al. 2010) and summer (21 Dec) insolation (W/m²) at 60°S (Laskar et al. 2004). Calibrated radiocarbon ages and 1σ (black) and 2σ (grey) age ranges for Canopus Hill and Lago Guanaco are plotted at the base of the respective panel. Note that PAR and CHAR have both been capped at the modern end due to high accumulation rate. The grey boxed area marks the transition period during which the ASL strengthened over the South Atlantic.